The Structure of Microsolvated Benzene Derivatives and the Role of Aromatic Substituents

Bernhard Brutschy*

Institut für Physikalische und Theoretische Chemie, J. W. Goethe-Universität Frankfurt, Marie-Curie-Str. 11, D-60439 Frankfurt a. M., Germany

Received February 14, 2000

Contents

Bernhard Brutschy was born in Waldshut/Baden-Württemberg, Germany, 1946. He received his diploma in Physics at the University of Freiburg in 1973 and his Ph.D. degree in 1977, working with Professor H. Haberland on elastic scattering of electronically excited helium. After this he held a postdoctoral position at the Hahn-Meitner Institut in Berlin with Professor Henglein. In 1978 he moved to the Freie Universität Berlin to work with Professor H. Baumgärtel at the Institute for Physical and Theoretical Chemistry, where he worked both with synchrotron radiation from BESSY and with pulsed lasers to study the energetics and dynamics of molecular clusters. In 1992 he became Full Professor at the J. W. Goethe Universität in Frankfurt/Main, Germany. His main research interests include experimental studies on the structure and reaction behavior of vdW complexes, sampled both with UV/IR nanosecond and picosecond pump−probe laser techniques, and analytical chemistry by laser desorption of ions of large biomolecules from liquid beams.

I. Introduction

Molecular clusters are nowadays preferred model systems to study both the energetics and dynamics of molecules in a tailored molecular environment.[1−5] For the physical chemist they may serve as "nano-test tubes" to investigate complex chemical reactions from a molecular point of view.[6−12] Van der Waals (vdW) clusters are advantageous model systems since their size, content, and sometimes their structure may be varied more or less at will. Thus, the electronic properties of an atom or a molecule may be investigated in the transition from isolation to solvation or generally to the condensed phase, with hitherto unprecedented levels of detail.[13,14] Many phenomena, otherwise exclusively observed in the liquid phase, such as solvent-mediated chemical reactions,[7,15,16] cage effects,[17−19] etc., are amenable to a detailed spectroscopic study and often to a real-time analysis of the dynamics. Since the molecular clusters are produced in supersonic beams, i.e., in the gas phase under collision-free conditions, they are free of perturbations from many-body interactions or macromolecular structures inherent for molecules in the condensed phase. The spectroscopic characterization of these model systems of reduced complexity also allows their study by high-level ab initio simulations and one to cross-check the accuracy of the latter by comparing experimental and theoretical results.

The following contribution highlights recent advances in the methods used to characterize the energetics and structures of microsolvated species. One treated in more detail is an IR/UV double-resonance method. It allows the vibrational spectros-

* To whom correspondence should be addressed. Telephone: +49 69 798 29587. Fax: +49 69 798 29560. E-mail: brutschy@chemie.uni-frankfurt.de.

10.1021/cr990055n CCC: $35.00
Published on Web 10/05/2000

copy of size-selected clusters in their electronic ground state. Its potential is illustrated by the results concerning the subject of this article, i.e., the ways how substituted benzene molecules are microsolvated by protic solvents. The term microsolvation means the more or less specific binding of n polar solvent molecules ($n < 5$) on the aromatic chromophore. Those substituents are dealt with in greater detail, as they are only weak hydrogen bond donors or acceptors or even unable to form any H-bond. The main objective was to discuss the influence of +I and −I groups, respectively, on the strength of the weak H-bond between one or several OH solvent donor groups and the aromatic π-system. An important issue will be to identify the major binding sites and the different types of weak hydrogen bonds (H-bonds) and thus to illustrate the hierarchy and topology of different H-bonds already encountered in such a simple model system. These results are supplemented by the findings from microsolvation studies, where the substituents are strong H-bond donors and acceptors taking part in the H-bonding network of the solvent moiety. Thus, H-bonding to the π-system is often negligible for these chromophores.

The experimental methods utilized to derive a majority of the results presented are as follows: (1) supersonic beams to form ensembles of mixed vdW clusters of different size and composition; (2) laser-induced resonant two-photon ionization spectroscopy (R2PI) to select a particular cluster size from the beam and subsequently mass analyze it in a time-of-flight (TOF) mass spectrometer; and (3) infrared (IR) predissociation spectroscopy to characterize its structure before or after the ionization. Also, alternative methods to study the structure of microsolvated molecular ions will be discussed in the survey on modern spectroscopic methods.

The reasons for the restriction on the topic of the structure and energetics of microsolvated benzene derivatives are many. First, the author and his group have worked on this subject for the last five years and most of the results presented in the following have not yet been summarized in an overview article. However, this would not justify a review article if the discussed topics and applied methods presented would not be of considerable interest for future work in the field of molecular clusters and intermolecular forces. This is emphasized by the rapidly growing number of results from other groups working with similar or related techniques. A further strong motivation stems from the fact that other review articles in this issue present complementary results on similar or different H-bonded molecular systems. Some of the contributions from the theoretically working groups address these cluster systems and their intermolecular bonds from first principles theory. Due to significant progress in computational methods and the increased availability of supercomputers, molecular aggregates of reduced complexity can now be studied theoretically at a sufficient level of accuracy to allow the comparison with spectroscopic results. Thus, the new link between experiment and ab initio theory provides an unprecedented depth of analysis, which would never be available by only experiment or theory alone. The benefit from such a joint effort is a more accurate description of intermolecular forces and clearer concepts on microsolvation, which are crucial both for a qualitative understanding of solvation phenomena and for the molecular modeling of species in solution. A better understanding of the structural features of large biomolecules may also emerge from such case studies.

The interest in the structure of microsolvated substituted benzenes is also motivated by their relevance. Substituted benzenes are ideal chromophores to investigate solute−solvent interactions and, in particular, hydrogen-bonding networks (H-bonding) in great detail and selectivity by applying multiresonance laser spectroscopy. The subtle interplay of electrostatic and dispersive interactions and of hydrophilic and hydrophobic forces between an aromatic molecule and a polar solvent environment may be investigated in a systematic manner. Moreover, benzene and substituted benzenes are archetypical molecules in organic chemistry. To understand the effect of the substituent on the overall intermolecular binding behavior of these molecules is of fundamental importance for the understanding of the aromatic−hydrophilic attraction of more complex derivatives. The latter are encountered in many natural chemical systems and reactions. These range from the tertiary structure and functions of the molecular building blocks of life, i.e., of proteins and oligonucleotides, to atmospheric aerosols.[20] Many binding motifs such as cation−π,[21] amino−aromatic,[22] and polar−π interactions[22] are crucial in molecular recognition and conformational folding dynamics. They determine the interaction of phenyl residues of the aromatic amino acid triad phenylalanine, tryptophan, or tyrosin in aqueous solution.

Quite a large number of review articles[23−29]and monographs[30−32] have been published in recent years on vdW clusters in general, from which three thematic issues in *Chemical Reviews* should be mentioned.[33−35]

In the context of the restricted subject of this report, special attention should be given to the reviews by Zwier,[25] mainly on microsolvated benzene, and by Ebata et al.,[36] mainly on microsolvated hydroxybenzenes. Hence, the results on these systems are only discussed in a reduced way and only when necessary for the discussion of the topics of this review.

Many of the experimental results presented in the following on substituted benzenes microsolvated by water or methanol could only be fully analyzed in close collaboration with the groups of K. S. Kim and P. Hobza. The theoretical and methodical aspects of their computational contributions will be presented in their respective articles in this issue.

In the following, first an overview of the experimental methods used to study the structure of molecular clusters—neutral or positively ionized—will be given together with a critical evaluation of their potentials and limitations. Then results on the structure and vibrational spectroscopy of microsolvated substituted benzenes will be presented. The latter are singly/doubly methylated or fluorinated benzenes,

microsolvated by up to four water (W) or methanol (MeOH) molecules. The two types of substituents change the charge in the aromatic π-system in a particular way: while methyl substituents are electron-donating, fluoro substituents are electron-withdrawing relative to hydrogen.[37]

The structure of the solvent environment of the chromophore is determined by the interplay of different intermolecular forces: H-bonds among the solvent molecules and H-bonds or dispersive interactions of the solvent moiety with the π-electron system or polar substituents of the aromatic chromophore. From characteristic vibrational fingerprints of the cluster, structural assignments will be deduced, which will be checked by comparison with results from ab initio calculations by Tarakeshwar and Kim.[38,39] The good agreement of the results from spectroscopy and ab initio simulation justifies a further analysis of the nature and strength of the contributing intermolecular forces. This is necessary to get a qualitative understanding of what determines the structures and binding energies of such complexes.

Spectroscopic results on a special type of H-bond first discussed by Hobza et al.[40] termed "improper, blue-shifting hydrogen bond" and formerly called "anti-hydrogen bond" will supplement the topic on H-bonds in such solute−solvent model systems.

In the last part, this article tries to give a short overview on results of microsolvated benzene derivatives, where substituents such as OH and NH_2 are able to form strong H-bonds to the solvent moiety. A summary and a discussion of future perspectives will close the survey.

II. Experimental Methods

A. Cluster Production

Molecular clusters are usually produced in continuous or pulsed supersonic beams.[41] To obtain both an efficient cooling rate and formation of vdW clusters, the seeded beam technique is applied. To synthesize, for example, heterogeneous solute−solvent clusters of type $A{\cdot}B_n$, the component gases A (chromophore) and B (solvent) are mixed at relative concentrations of typically less than 1% with a seed gas. As seed gas helium or argon is used; however, if particularly efficient cooling is needed, a mixture of helium and neon is preferable.[42] This gas mixture is expanded at high pressure through a tiny nozzle, with a typical diameter of 100 μm, into high vacuum. If the solute and/or solvent are liquid at room temperature, a gas mixing station where the seed gas is doped with the sample gases is mandatory.[43]

For the widely used pulsed nozzle sources (pulsed valves), an inhomogeneous cluster size distribution is observed both in the temporal and spatial profile of the gas pulse.[44] Generally, monomers and smaller clusters appear at the beginning and at end of the gas pulse while larger complexes show up in its center. The overall spatial profile of the cluster size distribution in the gas pulse is, thus, more or less symmetrical to the beam axis.

The observed cluster size distribution may be controlled within certain limits by varying experimental parameters such as (1) the length of the opening pulse of the valve, (2) the mixing ratios of the gases and the stagnation pressure of the gas mixture, and (3) the part of the gas pulse sampled with the cluster detection method. Solid compounds are evaporated in heated nozzle sources, thus allowing the seed gas to pick up their vapor.

The size distribution of the clusters may be determined by ionization combined with mass spectrometry. However, in the ionization process, in general, a considerable amount of excess energy is imparted to the clusters. This energy may be easily dissipated into the dense manifold of intermolecular, vibrationally excited states of a cluster, causing it to dissociate.[45] This process of evaporative cooling of the cluster is henceforth termed "vdW fragmentation" (vdWF). It is responsible for the fact that the ion signals observed in a mass spectrum are often "contaminated" by the fragmentation of larger complexes. For a more detailed description of a typical experimental setup, the reader is referred to examples described in the literature.[8,41]

B. Selective Cluster Detection and Structural Analysis

By means of the methods described above, neutral clusters are produced in a more or less broad size distribution, the width of which depends sensitively on the expansion parameters. Hence, the study of a cluster of a certain size and, in particular, the investigation of its structure necessitates a size-selective detection method. In the last 20 years several methods have been developed and applied.

Apart from cluster separation by elastic scattering[45] (see also the article of Buck and Huisken in this issue), access to individual molecular cluster sizes is only provided by different spectroscopies.

A classical spectroscopic method to determine the structure of a vdW cluster is Fourier transform microwave (MW) spectroscopy.[46−52] It allows the investigation of specific neutral clusters even in mixtures of different cluster sizes without the need for mass selectivity just by identifying the rotational transitions of individual vdW complexes. Because of the growing complexity in the spectra of larger clusters, mostly binary complexes of small molecules have been studied in the past with this method.

The most widely used methods nowadays are different laser spectroscopic methods which provide mass selectivity. Aside from a size-specific detection, they also allow one to derive information about the structure of a cluster. Ionization and laser-induced fluorescence methods in addition provide insights into the reactivity of clusters after their photoexcitation or ionization.

A very powerful technique to determine the structure of smaller clusters is rotationally resolved optical spectroscopy.[24,28] The article by Neusser in this issue will review the recent progress achieved with this technique. However, it is limited by the size of the species feasible for a spectroscopic analysis. For larger molecules or clusters, such as phenol dimer,

the rotational constants becomes so small that the rotational transitions, measured in the frequency domain, can no longer be resolved.

In the following, some spectroscopic methods will be described in more detail because they are either the central methods which have been utilized to derive most of the results discussed in this article or because of their future potential in this field.

1. Rotational Coherence Spectroscopy (RCS)

A very promising structure-sensitive method is rotational coherence spectroscopy (RCS) developed by Felker and co-workers.[23,53] It allows for the determination of the rotational constants of jet-cooled species in the electronic ground and excited states. Its future potentials will probably dramatically increase with the new generation of picosecond laser systems now available.

In RCS, the thermally averaged rotational quantum beats of a coherently populated state of a cluster/molecule are measured in the time domain with picosecond time resolution. For species that are not too large, its accuracy intrinsically increases with the size of the system, i.e., with a decreasing rotational velocity. It is the preferred method to determine the rotational constants of larger aromatic molecules and their clusters both in the S_0 and the S_1 state. Since the rotational constants do not provide the structure, additional calculations are necessary to track down the structure of the complex.

The most frequent implementation of RCS is time-resolved fluorescence depletion spectroscopy (TRFD). In its simplest configuration, two picosecond laser pulses with identical wavelengths and polarizations, but separated in time with a variable time interval, interact resonantly with the clusters in the beam (one-color RCS). The pump pulse produces a coherent population of species in the electronic ground and excited states with the transition dipole moment aligned along the polarization axis of the laser light. The equally polarized probe pulse analyzes this initial alignment at later times by inducing the reverse transition at variable time delays. Due to the rotation of the molecules, however, the alignment is destroyed after the time zero but recovers periodically up to time intervals of several nanoseconds. A realignment is detected by the probe pulse by an efficient pumping of population from the S_0 to the S_1 or vice versa. This results in a change (dip or enhancement) in the isotropically emitted fluorescence signal. As a function of the delay between both pulses, one then observes in the fluorescence yield a spectrum of regular transients, from which the rotational constants may be derived by calculations with high precision.[54] A two-color pump−probe scheme allows for the determination of the transients in S_0 and S_1 separately by time-resolved stimulated Raman-induced fluorescence depletion (TRSRFD) and time-resolved stimulated emission pumping (TRSEP).

With a larger size distribution of clusters, each excited species contributes to the measured total fluorescence signal and their transients will be superimposed in one trace. Since the relative depletion often amounts to less than 1%, the transients are easily blurred by noise. Hence, for larger size distributions, this fluorescence depletion method suffers from several shortcomings, among which the most significant one is the missing mass selectivity. Selectivity is only achieved if a cluster-specific UV transition is excited in the sampled species. Since in larger clusters spectral specificity is often lacking, this method then forfeits mass selectivity. Hence, only small aggregates from narrow size distributions have been studied in this manner up to now. Other limitations may be the selection rules in this process, which sometimes prevent the determination of a complete set of rotational constants. The implementation of RCS with time-resolved ionization detection (TRID) of the excited state[23] circumvents a lot of these problems and incorporates mass selectivity. Up to now, two excitation schemes are known in the literature[55−57] which allow mass-selective RCS. A summary of the clusters, studied with RCS, may be taken from Felker[58] or Topp.[59] Typical examples are the results on phenol dimer,[60] fluorene−benzene dimer[61] on Ar_3^+,[62] on complexes of perylene with water or alcohols,[63] or on 9,9′- bianthryl with Ar and water,[64] or the structure of pDFB·Ar in the S_0 and S_1 state.[65]

2. Resonant Two-Photon Ionization (R2PI)

A very sensitive and mass-selective detection method widely used nowadays to study clusters is resonant two-photon ionization (R2PI).[66,67] It is easily implemented by using tunable pulsed nanosecond

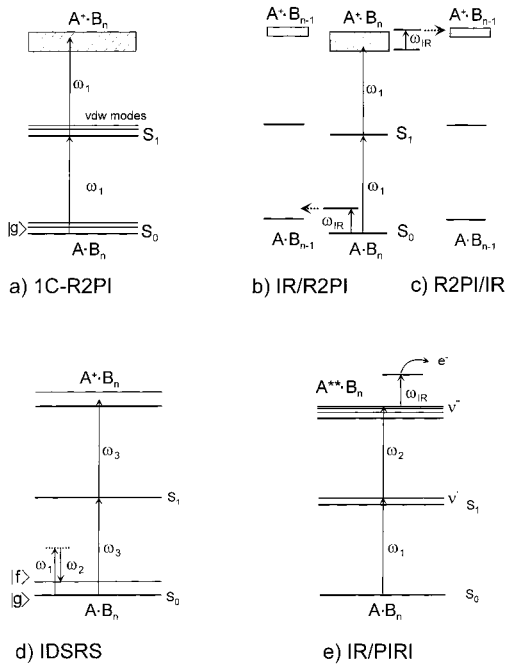

Figure 1. Excitation schemes of double- and triple-resonance spectroscopy applied for the measurement of vibrational spectra in the neutral and ionized vdW complexes. (a) 1C−R2PI: one-color-resonant two-photon ionization via the S_1. (b) IR/R2PI: infrared spectroscopy by predissociation of the neutral cluster, detected by R2PI. (c) R2PI/IR: infrared spectroscopy by predissociation of the cluster cation produced by R2PI. (d) IDSRS: ionization-detected stimulated Raman spectroscopy. (e) IR/PIRI: autoionization-detected infrared spectroscopy of clusters resonantly excited into Rydberg states by MATI.

lasers and time-of-flight (TOF) mass spectrometry. Since R2PI is the size-selecting part of the double-resonance vibrational spectroscopy discussed below, it is described here in more detail. It starts, for example, with a resonant $S_1 \leftarrow S_0$ transition in the aromatic chromophore A, followed by a nonresonant transition into the ionization continuum, as depicted in Figure 1a. For many chromophores laser light of one color (ω_1) is sufficient for both transitions (1C−R2PI); for others two separately tunable lasers are mandatory (2C−R2PI). The ion yield measured by scanning the wavelength of the excitation laser reflects the resonant part of this two-step process (R2PI spectrum).[8] Since the ultracold chromophore generally exhibits a discrete absorption spectrum, which is for the most part only weakly perturbed by few associated solvent molecules, the R2PI spectra of small clusters also exhibit discrete spectra which are very similar to that of the isolated chromophore.[68] The changes induced in a chromophore spectrum by attached solvent molecules are (1) band shifts, (2) additional spectroscopic features from intermolecular vdW vibrational modes, and (3) additional bands from isomeric cluster structures. The R2PI spectrum of a cluster represents more or less its optical absorption spectrum and may be viewed as a unique spectroscopic fingerprint.[68−70] The examples in Figure 2 show the R2PI spectra measured for some product ions of the cluster system fluorobenzene (FB)/methanol. The microsolvated chromophore FB was ionized via resonant transitions in the vicinity of the vibrationless $S_1 \leftarrow S_0$ ($\pi^*\pi$) 0_0^0 transition of the isolated chromophore. As illustrated by the appearance of anisole$^+$, aside from ionized clusters, also ions from intracluster reactions are observed. As will be discussed later, the spectral features observed in an ion channel may be assigned to specific neutral cluster precursors. For larger clusters, the R2PI spectra are often broad and congested and with bands at similar spectral positions. In this case cluster-selective ionization is no longer possible.

Clusters with one solute and n solvent molecules are termed in the following as 1:n clusters. A cyclic or linear structure is marked by the subscripts "cycl" or "chain". A complication of a R2PI spectrum may result from the fragmentation of larger clusters into several different product ions, induced by the ionization. This is due to the fact that after its ionization, the complex often suffers a structural rearrangement combined with vdW fragmentation or an ion−molecule reaction. The different product ions from one precursor exhibit identical fingerprints, allowing their classification. If some of the parent ions survive, the size of the neutral precursor may be assigned by mass spectrometry. If, however, the reaction or fragmentation processes are quantitative, this is no longer possible although the spectra of the product ions are still encoded with the R2PI fingerprints of the precursors. In general, the latter may not be utilized to assign the size or even the structure of a cluster. The shifts of the transitions measured for a microsolvated chromophore depend on the change of the binding energy in both the ground and excited states. With polar solvent molecules one generally

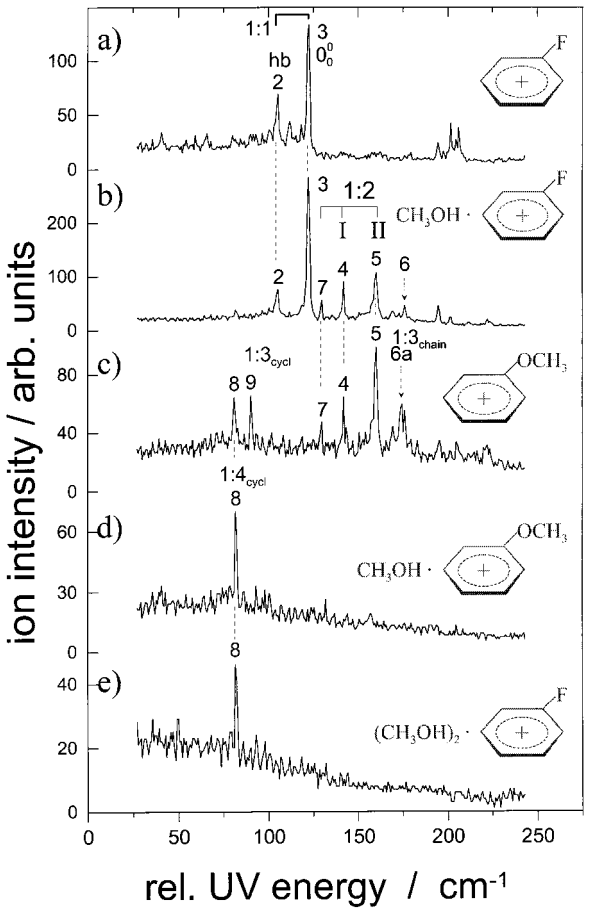

Figure 2. R2PI spectra measured for product ions of the cluster system FB·$(MeOH)_n$, $n = 1-4$ in the vicinity of the $S_1 \leftarrow S_0$ 0_0^0 transition of FB (ν_{00} = 37 818 cm^{-1}). The neutral precursor clusters are marked by 1:n (n = number of solvent molecules) (for further explanations, see text). The dashed lines represent the positions of the OH modes in isolated water dimer.

observes blue shifts, while with nonpolar solvents red shifts are observed. The intermolecular modes observed in an R2PI spectrum are likewise not very helpful. They pertain to the cluster with the chromophore in the S_1 state, for which ab initio calculations are still far away from being accurate enough for an unambiguous comparison of theory and experiment.

Due to the obstacles mentioned above, the R2PI spectra of product ions of quantitatively reacting or fragmenting clusters are in general not assignable. Exceptions are the fingerprints of clusters, which react in a particular manner, such as the cations of microsolvated toluene.[71] Here the ionized chromophore may stabilize to the benzyl radical by quantitatively transferring a proton to the solvent moiety of a certain minimum size. If this intracluster proton transfer is exothermic and induces the dissociation of the solvent moiety from the proton-donating cation, without fragmenting the protonated species itself, the latter is detected intact in the mass spectrometer. Early studies of such dissociative proton-transfer reactions (dPT)[71,72] substantiated that protic solvent molecules form subclusters attached to the aromatic chromophore.

The predominance of subcluster formation for protic solvent molecules is a consequence of the different strength and nature of the intermolecular bonds. The more hydrophobic solute−solvent interaction is often considerably weaker than the hydrophilic intersolvent interaction. The macroscopic consequence of this mismatch is the spurious solubility or even immiscibility of many benzene derivatives in water or alcohols.

3. IR/R2PI Ion-Depletion Spectroscopy (IR/R2PI)

The favorite method to probe the vibrations of the solvent and solute moiety of a cluster of type $A{\cdot}B_n$ is a double-resonance laser spectroscopy termed IR/R2PI ion-depletion spectroscopy, henceforth abbreviated by the acronym IR/R2PI. Its excitation scheme is depicted in Figure 1b. Its principle is simple. If a mid-infrared (IR) laser beam excites an energetic intramolecular vibration of a mixed cluster, such as the OH stretch of water or an aromatic CH vibration of the chromophore, the cluster decays very rapidly by IVR and vibrational predissociation. If the population of the cluster beam is probed some 100 nanoseconds afterward by R2PI, all product ions, originating from the IR-absorbing cluster species, will exhibit a common depletion in the ion yield. Hence, it is a hole-burning spectroscopy.[73,74] By keeping the wavelength of the UV probe laser fixed on a cluster-specific R2PI fingerprint band while scanning the wavelength of the IR laser, an ion-depletion spectrum is observed. It represents more or less the IR absorption spectrum of the neutral cluster before it is ionized by R2PI. Thus, even different cluster sizes with accidentally coinciding R2PI fingerprint bands can be distinguished unequivocally. The method combines the highly selective and sensitive ionization detection of R2PI mass spectrometry with the structural sensitivity of vibrational spectroscopy in the mid-IR region.

In a typical experimental setup the IR pump laser beam is superimposed coaxially and antiparallel to the beam axis[8] and hits the gas pulse just behind the skimmer. The pulsed probe laser beam crosses the molecular beam at right angle in the ionization zone of a TOF mass spectrometer.

As light sources for tunable coherent radiation in the mid-IR spectral region, one nowadays uses a difference frequency mixer[75] or a seeded optical parametric oscillator (OPO).[76,77] An OPO employs nonlinear, birefringent crystals (viz. $LiNbO_3$) which can be added on as an external component to a pump laser, typically a Nd:YAG laser. It contains a cavity and splits the energy of a photon between two photons, termed signal and idler, both at longer wavelength. The energy ratio between the photons, and thus the resulting wavelengths of each, is changed by varying the angle between the axis of the pump radiation and the optical axis of the crystal. The resulting bandwidth of the low-energy idler component, typically used in studies in the mid-IR, is some 6− 10 cm^{-1}. It can be reduced by more than an order of magnitude by utilizing injection seeding[77] or a dispersive element in the resonator. A state of the art seeded IR OPO has a typical bandwidth of 0.2 cm^{-1}, a tuning range from 2.6 to 4 μm, and pulse energies of 2−10 mJ/pulse.

The IR predissociation spectroscopy was first applied in Lee's group[78] to study the vibrational spectra of non-size-selected water clusters. Later Huisken et al.[79] implemented size selectivity by combining it with Buck's scattering method. It is was also used to study the structure of microsolvated ions.[80−84]

In combination with R2PI, i.e., as IR/R2PI, it was first used by Page et al.[85] to study the IR spectrum of the benzene monomer and dimer in the region of the aromatic CH vibrations.

Riehn et al.[86,87] first applied IR/R2PI as a method to study and characterize a microsolvation environment in a cluster. The cluster investigated consisted of fluorobenzene microsolvated by an unknown number of methanol molecules. It quantitatively decayed after R2PI into the ion channels fluorobenzene$^+{\cdot}$(methanol) and anisole$^+$, as illustrated in Figure 2. Anisole$^+$ was produced in a nucleophilic substitution reaction (S_N2) in the ionized complex. Since both ions showed identical fingerprint bands in their R2PI spectra, a common precursor was evident, but its identity and in particular its size was first under discussion.[88,89] Interrogated by IR/R2PI in the region of the CO stretch of methanol by utilizing a CO_2 laser, the depletion spectra of both ions revealed two absorptions, nearly identical to those of the free methanol dimer recorded by Huisken et al.[90,91] Thus, the association of a methanol dimer to the chromophore, i.e., a 1:2 neutral precursor, could be assigned unambiguously. Interestingly, the CO vibration frequency of the acceptor molecule of the dimer exhibited a small blue shift as compared to that in the free methanol dimer. The latter was rationalized by the formation of a hydrogen bond between the methanol dimer and the chromophore. These results were later confirmed by IR/R2PI in the OH stretch region both by Fujii et al.[92] and Djafari et al.[43] Two main advantages of this new type of cluster spectroscopy became immediately apparent from this study: first, the possibility of determining the size and structure of the solvent subcluster even in the case where it was destroyed quantitatively by the detection process and, second, the possibility of recording spectral hole-burning spectra (SHB). The latter were recorded by keeping the wavelength of the IR laser fixed on a vibrational transition of a cluster while tuning the wavelength of the UV probe laser.[87] The hole-burning spectra obtained differed from the normal R2PI spectrum of a product ion by the depletion of all UV fingerprints pertaining to a common IR absorber. With this method, all spectroscopic features originating from fragmenting larger clusters, isomers, or hot bands can clearly be identified. Hence, the IR/UV hole-burning spectroscopy is particularly useful with fragment contaminated R2PI spectra, typical for vdW clusters.

If the intermolecular interaction in a cluster strongly changes the frequencies and intensities of the vibrations of some of its components, as typical for molecular groups involved in hydrogen bonding,[93] this spectroscopic information may be used to unravel its structure. It may often be analyzed in a straightfor-

ward manner, particularly when the knowledge, accumulated over the years by IR spectroscopy in matrixes[94] and in the condensed phase,[95,96] is taken into account. Nowadays the experimental vibrational spectra may be compared with the vibrational frequencies obtained from high-level ab initio calculations.

In summary, the advantages of two-dimensional IR predissociation/resonant two-photon ionization spectroscopy are manifold. (1) The combination of the very high sensitivity and mass selectivity of R2PI with IR vibrational spectroscopy allows the deduction of the structure of small clusters available only at very low number densities. Thus, the method still works when alternative absorption methods[97] fail or forfeit mass selectivity. (2) Bands from isomeric structures, hot bands, and spectral features from fragmenting larger complexes, complicating an R2PI spectrum, may be distinguished and often assigned in a straightforward manner. (3) Even in cases where R2PI spectra exhibit broad, congested bands, clear spectroscopic IR fingerprints are often obtained by IR/R2PI.

In recent years, impressive results concerning the structure of microsolvated chromophores have been deduced with this method. With the advent of tunable IR−OPOs and difference frequency mixers, mainly the OH and CH stretches of both the solvent and solute moiety have been monitored. These IR spectroscopic studies of clusters are in direct relation to analogous studies in the condensed phase[93,95] where these interaction-sensitive modes have been utilized as indicators of the strength and type of H-bonding and basicity,[98−101] respectively. Various groups have applied IR/R2PI to investigate H-bonding in microsolvated benzene derivatives. Mikami and collaborators[102] first investigated the OH stretches of phenol·(water)$_n$ clusters (n = 1−3). Zwier and co-workers studied the cluster system benzene·(water)$_n$ (n = 1−9).[103] The results derived by these and other groups will be discussed in greater detail below.

With the increasing number of groups utilizing IR/R2PI, the designation and acronyms proposed for it also increased nearly linearly with the number of groups. This really confusing situation should be dismissed in favor of one designation. The different acronyms used in the literature and listed in Table 1 shall be enumerated for completeness in the following. Zwier's group proposed and use RIDIRS (resonant ion-dip infrared spectroscopy),[103] Mikami's group IDIRS (ionization-detected infrared spectroscopy),[36] while others proposed IR−UV SHB (infrared−ultraviolet spectral hole burning)[104] or simply IR−UV ion-dip spectroscopy.[105] While some of these alternative acronyms are only marginally shorter than IR/R2PI, they no longer refer to the essential part of the method, namely, the cluster selectivity achieved by R2PI. Hence, in the following we use the originally proposed acronym IR/R2PI. Mikami and collaborators also recorded fluorescence-dip IR spectra of microsolvated chromophores.[106] While this methodical simplification forfeits mass selectivity, the selective excitation of a cluster is nevertheless possible, provided the UV-absorption fingerprints are unique to the species studied and are known un-

Table 1. List of Acronyms

a. Compounds

AN	aniline
ANI	anisole
BZ	benzene
BN	benzonitrile
CLB	chlorobenzene
Cf	chloroform
EtOH	ethanol
FB	fluorobenzene
Ff	fluoroform
IN	indole
pCLFBZ	*p*-chlorofluorobenzene
pDFB	p-difluorobenzene
PH	phenol
PX	*p*-xylene
MeOH	methanol
1MIN	1 methylindole
3MIN	3 methylindole
TO	toluene
W	water

b. Methods, Processes, Etc.

A	acceptor
ADIR (IR/PIRI)	autoionization-detected infrared absorption
BSSE	basis-set superposition error
CT	charge transfer
D	donor
D/A	donor−acceptor
DFT	density functional theory
dPT	dissociative proton transfer
FDIRS	fluorescence-detected infrared spectroscopy
FDSRS	fluorescence-detected stimulated Raman spectroscopy
HF/SCF	Hartree−Fock self-consisted field
IDSRS	ionization-detected stimulated Raman spectroscopy
IDIRS (IR/R2PI)	ionization-detected infrared spectroscopy
IR	infrared
IR−PARI	infrared photodissociation after resonant ionization
IR/PIRI	infrared predissociation spectroscopy detected by PIRI
IR/R2PI	infrared predissociation spectroscopy detected by R2PI
IR−UV SHB (IR/R2PI)	infrared-ultraviolet spectral hole-burning
IVR	intramolecular vibrational energy redistribution
LIF	laser-induced fluorescence
MATI	mass-analyzed threshold ionization
MP2	Møller−Plesset perturbation theory second order
MW	microwave spectroscopy
OPO	optical parametric oscillator
PIRI	photoinduced Rydberg ionization
π-OH	H-bond OH···π-system
R2PI	resonant two-photon ionization
R2PI/IR	infrared predissociation spectroscopy after R2PI
RCS	rotational coherence spectroscopy
RIDIRS (IR/R2PI)	resonant ion-dip infrared spectroscopy
σ-OH	linear OH···substituent H-bond
SHB	spectral hole-burning
S_N2	nucleophilic substitution reaction
UV	ultraviolet
vdW	van der Waals
TRID	time-resolved-ionization detection
TRSEP	time-resolved-stimulated emission pumping
TRSRFD	time-resolved- stimulated Raman-induced fluorescence depletion
TOF	time-of-flight
ZEKE	zero kinetic energy
ZPVE	zero-point vibrational energy

equivocally. The technique is of advantage when ionization is not easily achieved. For this method the acronym FDIRS (fluorescence-detected infrared spectroscopy) was used.

4. Ionization/Fluorescence-Detected Stimulated Raman Spectroscopy

When a cluster is vibrationally excited not by absorption of infrared light but by stimulated Raman scattering, a complementary depletion spectrum may be recorded. The first implementation of stimulated Raman spectroscopy detected by ion depletion was realized by Felker and collaborators,[107] who termed this method IDSRS (ionization-detected stimulated Raman spectroscopy). Its excitation scheme is depicted in Figure 1d. The vibrationally excited state is prepared by stimulated Raman scattering with the laser frequencies ω_1 and ω_2. The reduced population of the ground state is detected by R2PI. Felker et al. studied a variety of 1:1 complexes of phenol and substituted phenols with polar and nonpolar molecules and found that the phenolic CO and OH stretch fundamentals relax more efficiently by hydrogen bonding than do the other modes in the complex. Mikami and collaborators[108] detected the Raman scattering by fluorescence depletion. They studied the vibrational spectra of the C−C and C−N stretch of benzonitrile microsolvated by water and methanol. They termed this technique fluorescence-detected stimulated Raman spectroscopy (FDSRS). The spectra achieved with IDSRS or FDSRS are generally complementary to those recorded with IR/R2PI and in addition allow one to study vibrations not accessible by IR laser radiation.

5. Multiresonant Vibrational Spectroscopy of Ions and Ionized Clusters

By reversing the sequence of the IR and UV laser pulses, the vibrational spectra of clusters with the chromophore in the excited or ionized state can be determined (Figure 1c). In the latter case, the acronym R2PI/IR would be appropriate. Recently also the acronym IR−PARI (infrared photodissociation after resonant ionization) was proposed for this method.[75]

The first application of this technique was reported by Takeo and collaborators for solvated aniline.[109,110] A problem which has to be reckoned with when using this procedure is that often the vibrational spectra from a warm rather than from a vibrationally cold cluster ion will be sampled. In addition, the binding energy in an ionized cluster is generally considerably larger than in the neutral species, so that the IR absorption, detected via predissociation of strongly bound solvent molecules, results in preferential detection of the spectra from warm clusters. In the vibration spectra of the ionized complexes studied, the line width of the vibrational modes were much larger than those observed in the neutral complexes,[111] which was attributed to this problem. It may be avoided by studying the ionized clusters in an ion trap after cooling them by collisions with an inert background gas at low pressure.[112,113] An alternative method was developed by Johnson and coworkers.[84] They attached several argon atoms, as a sort of micromatrix, onto the ionic clusters, using these both as evaporative coolant and as "spy" or "messenger" molecules to detect the IR absorption by ion depletion. In R2PI/IR depletion spectroscopy, as just discussed, the vibrational state of the ion is in general not well defined. Remedial action is taken by a new triple-resonance spectroscopy. It combines IR absorption and state-selective population of ionic states by MATI spectroscopy[114,115] (mass-analyzed threshold ionization). The MATI part starts, as sketched out in Figure 1e, by a resonant transition from the electronic ground into a vibrationally excited state (ν') of the S_1 cluster, followed by a second resonant transition into long-lived, high-n, high-l Rydberg states (A**) of the cluster, converging to the ionization limit of a specific vibrational state (ν'') of the ionic core. While in the complementary ZEKE spectroscopy[116] the electrons produced after pulsed field ionization of these long-lived ZEKE-states ($150 < n < 300$) are detected (see the contribution from Dessent and Mueller-Dethlefs in this issue), in MATI spectroscopy the corresponding ions are collected. Hence, the method provides mass selectivity, which is of particular value if the ion undergoes a reaction.[117,118] To discriminate between the ions produced by field ionization of the ZEKE states and the likewise produced direct ions, the Rydberg molecules, giving the MATI signal, have to be separated from the direct ions by very small separation fields ($E < 1$ V/cm) in an ion-drift region before being field-ionized by the pulsed acceleration field in the TOF mass spectrometer. The ionic core of a cluster or molecule in such a Rydberg state is in a specific vibrational state, defined by the ionization threshold. Such a vibration excited with MATI is normally a low-frequency vibration of the aromatic chromophore.

If by absorption of a third photon the ion core is excited into an electronically excited state, the Rydberg electron autoionizes. Thus, by scanning the wavelength of a third excitation laser over the resonant transitions in the ion, the MATI signal of a species detected shows a characteristic depletion spectrum. This triple-resonance method, proposed and first applied by Johnson and co-workers to measure the electronic spectra of ions, is known under the acronym PIRI (photoinduced Rydberg ionization).[115,119] Recently Gerhards et al.[120] modified this method using a tunable IR laser for exciting high-frequency intramolecular vibrations in the ion. In this case the intramolecular OH and CH stretches are sampled in a frequency range of 3000 cm^{-1}. Since these are peculiarly sensitive to H-bond formation, they are a more specific fingerprint of the structure than the low-frequency modes, sampled by MATI/ZEKE. Thus, the vibrational spectra of two different isomers of resorcinol$^+$ (1,3-dihydroxybenzene) and the stretches of the solvent molecules in phenol$^+$·(H_2O) and indole$^+$·(H_2O) could be detected. In the latter cluster these did not couple with the intermolecular stretch and its overtone. A variant of this method, although without utilizing MATI spectroscopy, was applied by Fujii et al.[121−123] It was applied to study the OH stretching vibrations in molecules excited into the Rydberg states converging to the first ioniza-

tion threshold. Thus, a MATI-type separation of direct ions and Rydberg molecules, mandatory for states above the ionization threshold, was not applied and not necessary. Indeed, this study provided the first evidence that vibration-induced autoionization is observable for Rydberg excited species. The acronym ADIR (autoionization-detected infrared absorption) was proposed for this method. It was applied to determine the intramolecular H-bond for the ground-state cations fluorophenol$^+$ and methoxyphenol$^+$.

One problem of MATI or ZEKE spectroscopy should be pointed out, which is however intrinsic to any kind of ionization spectroscopy. Ionic vibrational states of a molecule or cluster may have very low Franck−Condon factors for a vertical two-photon transition starting from the neutral ground state. Unfortunately this is often the case with clusters such as benzene and its derivatives microsolvated by polar molecules. The reason for this is a strong conformational change induced upon ionization of the complex. As discussed below, in the neutral chromophore the protic solvent molecules are attached by H-bonds to the nucleophilic part of the aromatic molecule, i.e., either to the π-electron system or an electronegative substituent. In the adiabatic minimum of the ionic state, however, the solvent interacts with its lone pair electrons with the now positively charged aromatic ring. Hence, for these clusters no resonant MATI transitions could be found.[124] Only in cases where the polar molecule is strongly hydrogen bonded to a hydrophilic acceptor, preferably considerably away from the π-electron system, do both the ZEKE and MATI spectra show a resonance structure. This is the case for clusters of water with phenol (PH) and its derivatives[125,126] or for indole (IN) with water, i.e., IN·W.[127,128] Here the protic solvent molecules are relatively strongly H-bonded to the phenolic group[129−131] or to the N−H donor group of IN.[25]

This difference between weakly and strongly H-bound systems is illustrated by the binding energies of fluorobenzene (FB) and phenol with water. For the PH·W complex, a stabilization energy D_0 of 1929 cm^{-1} (5,5 kcal/mol) is calculated,[129] which compares with a considerably smaller binding energy of 938 cm^{-1} (2.68 kcal/mol) for FB·W.[38] In case of the PH$^+$·W, a structure very similar to that of the neutral complex was found by ab initio calculations.[75] Hence, in this and similar strongly bound clusters, IR/PIRI works well to study solvated cations, excited into specific vibrational states.

III. The Complexes

To illustrate the richness in structural information embedded in the IR/R2PI spectra, the article focuses in the following on weak H-bonds between several polar solvent molecules surrounding a substituted benzene molecule. The objective is to describe the role of electron-withdrawing and -donating substituents on the π-electron density in the aromatic ring and its consequences on the topology of microsolvation. To distinguish the substituent effect, first the results for benzene have to be considered.

A. Structure of Benzene Microsolvated by Water or Methanol

The question of the existence and nature of a bond between a water and benzene (BZ) molecule has stimulated a large number of studies in recent years. While it has been speculated for several years[132,133] that aromatic molecules can act as H-bond acceptors, experimental evidence increased within only the last 15 years.[134−136] The first studies with a detailed structural analysis were those of Suzuki et al.[137] on BZ·W and of Rodham et al.[48] on BZ·(ammonia). Gutowsky et al. [138] studied the BZ·W$_2$. The investigation of BZ·W established that water is bound to benzene via a π-OH H-bond, i.e., with the water positioned above the ring, pointing with its hydrogen atoms toward the π cloud.

While the structures of 1:1 and 1:2 clusters could be investigated by microwave spectroscopy, the larger complexes necessitated mass selectivity of the spectroscopic method, as provided by IR/R2PI. As already mentioned, the first detailed IR/R2PI spectra of the cluster systems of benzene microsolvated by water BZ·W$_n$ or methanol BZ·(MeOH)$_n$ were recorded by Zwier's group.[103,139] Since these results have been reviewed recently,[25] the reader is referred for more details to this review article. Since the following discussion focuses on the structure of microsolvated benzene derivatives, only the main points from this spectroscopic analysis with benzene shall be summarized here.

The IR/R2PI spectra of the BZ·W$_n$ system have been recorded in the region of the OH stretches of water from 3000 to 3800 cm^{-1}. The following information could be extracted from these spectra and from the spectra of isolated water clusters.[140,141] (1) When attached to benzene, medium-sized subclusters W$_n$ of water with $n < 6$ exhibit a similar structure to the analogous isolated water clusters, i.e., for $n =$ 3−5 they form H-bonded rings. (2) Due to the more local character of the OH vibrations of the water molecules forming H-bonded linear or cyclic subclusters, the observed vibrational modes can be divided mainly into two groups: H-bonded acceptor molecules (A) retain more or less the symmetric (ν_1) and antisymmetric (ν_3) OH stretch modes of water ((ν_{1A}) (ν_{3A})), corresponding to a linear superposition of the two degenerate local OH stretches of water. In donor water molecules (D), on the other hand, a H-bond is formed with one of these OH groups. Hence, the degeneracy is removed and the normal modes now retain a more local character. In the region of the ν_3 stretch of water, the stretches from free donor OH groups (ν_{fD}) appear, while on the low-frequency side of the ν_1 the stretches of the bound donor OH groups (ν_{bD}) appear. Therefore, the vibrations at higher frequency correspond to those of the dangling OH bonds and those on the red side to the H-bonded groups. If water acts both as donor and acceptor (D/A), the absorption bands of the bound donor OH groups $\nu_{bD/A}$ show a reduced red shift as compared to that of pure donor molecules. (3) If several water molecules are forming cyclic or linear subclusters via H-bonds, the normal modes consist of coupled local OH vibrations. Thus, it has been shown by

theory[140,142−147] that in isolated cyclic water clusters, the vibrations of the H-bonding OH groups in the ring are delocalized ring OH modes. Some of these for symmetry reasons exhibit low IR activity[79,148] or are degenerate in frequency. If these clusters are interacting with an aromatic chromophore, the normal ring modes are perturbed and split in energy, getting a more local character. At the same time their transition dipole moments increase, resulting in bands of comparable magnitude for each ring mode. Also at the same time the width of the bands increase. For larger cyclic clusters, these ring modes shift further to the red. (4) The number of resolved OH modes is approximately equal to the total number of OH bonds. As will be discussed later, this statement has to be taken with prudence. In the case of BZ·W_4, it proves wrong. Also, in some cases additional combination modes with intermolecular vdW vibrations are observable. Thus, the number of modes is only a first indication of the size of the complex. (5) In the group of the nearly isoenergetic free OH modes assigned to the "dangling bonds", a more red-shifted band appears, which is assigned to the vibration of the OH group, forming a π-OH "anchor" H-bond to the chromophore. Thus, strictly speaking, it no longer belongs to a free OH dangling bond. (6) In larger clusters, starting with BZ·W_6, indications for a change from a cyclic to a three-dimensional, hydrogen-bonded network is observed,[103,149] which is also found by theory for the isolated water hexamer.[150] Here several bands appear between the position of the donor bands for single H-bonds and the π-OH donor band, which are assigned to double-donor molecules. Their appearance signals a change in the coordination of the water molecules. (7) BZ·W_8 clusters take on two isomeric structures[151] with cubic water octamers of S_4 and D_{2d} symmetry, respectively, attached to the aromatic ring by a π-OH type H-bond. This ice-like structure is similar to the free water octamer studied by Buck et al.[152] In Bz·W_9 clusters, two isomers of W_9 with an expanded-cube structure are attached. In both, the ninth water molecule is inserted into one of the edges of the cubic water octamer, thereby deforming the latter.[152,153]

The benzene/methanol cluster system shows many parallels to that of benzene/water. Pribble et al.[139] found by IR/R2PI spectroscopy and ab initio calculations that again π-OH H-bonding between the benzene ring and a methanol subcluster dominates the solute−solvent interaction for $n < 4$. For $n = 4-6$, cyclic methanol clusters are formed.

The following differences between the microsolvation structure with methanol and water are notable: (1) Whereas an isolated methanol trimer has a cyclic case structure[154,155] analogous to a water trimer, in the BZ methanol forms a linear chain.[139] Thus, a π-OH H-bond obviously stabilizes a linear cluster more than an additional H-bond in a strained cyclic trimer. (2) Since methanol possesses only one OH group, all cyclic methanol clusters ($n > 3$) have no free OH groups. In this case no additional π-OH H-bond between the solvent ring and the chromophore is possible. Hence, their interaction with the aromatic molecule should mainly be of dispersive nature favoring a sandwich-type structure.

The BZ·$MeOH_n$ ($n = 1-5$) cluster system has also been studied by Gruenloh et al.[156] in the region of the CH stretches of methanol both by IR/R2PI spectroscopy and by ab initio calculations. They could extract the following data from the spectroscopic features of this vibrational mode. (1) The direction of the shifts of the OH modes in a methanol molecule is usually mimicked by the three C−H modes ν_3, ν_2, ν_9 of the methyl group. Generally, a red shift is encountered for a CH mode when the methanol acts as a hydrogen donor and a blue shift or a combination of blue and red shift if its acts as an acceptor. (2) Although the magnitude of the shifts induced by H-bonding is smaller than for the OH modes, the shifts are systematic.

Results on the structure of ternary water−methanol−benzene clusters have been reported by Hagemeister et al.[157] The clusters BZ·W_n·$MeOH_m$ (with $n + m = 4, 5$) exhibited in the IR/R2PI spectra the signature of H-bonded solvent cycles which are bound to benzene via a π-OH "anchor" H-bond. Several isomers of these ternary clusters have been predicted by theory at the DFT−B3LYP/6-31+G* level, but far fewer isomers were observed experimentally.

In addition to the experimental results with methanol, Zwier's group together with others[158−160] substantiated the spectroscopic analysis by ab initio calculations, mainly at the DFT-B3LYP/6-31+G* level. Since the review article of Kim et al. in this issue will treat the theoretical and computational aspects of such simulations in detail, the reader is referred to their review for a more in-depth discussion.

B. Structure of Substituted Benzenes Microsolvated by Water and Methanol

In clusters of substituted benzenes microsolvated by water or methanol, a detailed inspection of the substituent effect on the binding energy and binding site of solvent molecules is possible. As known from chemistry textbooks, methyl groups belong to electron-donating and halogens to electron-withdrawing substituents. Both types of substituents should thus change the electrostatic interaction of a polar solvent subcluster with the π-system. In the case of halogen substituents, their lone-pair electron orbitals represent additional polar binding sites. Thus, both σ-type H-bonds to the halogen X and alternative π-type H-bonds to the aromatic ring are possible. In addition, the strong intersolvent H-bonds play a crucial role. Thus, a cyclic methanol trimer, for example, is stabilized by three H-bonds and the dispersive interaction with the chromophore. A chainlike methanol trimer, however, is able to form a H-bond to different binding sites of the aromatic chromophore. Hence, the relative abundance of isomers with ring- or chainlike methanol trimers attached reflects the strength of the H-bonds to different binding sites of the chromophore in relation to the O···HO hydrogen bond in a strained ring geometry augmented by the dispersive interaction energy with the chromophore.

An indicator of the bond strength is the magnitude of the frequency shift of the OH vibration of the donor

group. As a first approximation, a larger red shift of the vibration of the bound donor group is correlated with a stronger H-bonding interaction.[99,100] However, this rule holds true only when the H-bonds compared are of a similar type.[161,162] The H-bonding induced red shift itself corresponds to a weakening of the OH bond induced by a partial charge delocalization from the acceptor's HOMO into an antibonding orbital of the OH group of the donor.[99,163]

Substituted benzenes not only provide a framework to study the subtle interplay of these different interactions, but they are also exciting model systems to study ion chemistry under various degrees of microsolvation with different solvents. This is due to the fact that the cations of substituted benzenes, when embedded in polar solvent molecules, in contrast to BZ^+ are very reactive.[8] The cations of halogenated benzenes (Ph−X) microsolvated by protic solvents may undergo nucleophilic substitution reactions (S_N2) with $X^\bullet$ or HX as leaving groups. These reactions, although exothermic already in a 1:1 cluster, are kinetically hindered and start only if the solvent subcluster possesses a minimum size. The cations of methylated benzenes, on the other hand, act as proton donors, i.e., as Brønsted acids. For toluene$^+$ (TO^+) and *p*-xylene$^+$ (PX^+) one observes a dissociative proton transfer (dPT) to the solvent moiety. The only precondition for this reaction to occur is that the proton affinity of the latter is larger than that of the conjugated bases of the cations, i.e., the benzyl or the methylbenzyl radicals.[71,164,165]

Before going further into the spectroscopic details of the microsolvated methyl- and fluorobenzene derivatives, some remarks on the behavior of other prominent substituted benzenes such as benzonitrile (BN) and phenol (PH) should be added. The cations of phenol show a similar dPT starting from a minimum size of the subcluster.[113,166−168] The microsolvation structure, however, is different from that of methylated or halogenated benzenes. Because of their hydroxyl group, hydroxybenzenes are incorporated directly into the structure of a H-bonding network of the solvent. Thus, in $PH{\cdot}W_{n=2-5}$, for example, the chromophore's hydroxyl group takes part in the formation of a H-bonded ring of water molecules.[36] Hence, the interaction with the solvent is dominated by this strong hydrophilic group. Mikami and collaborators studied many microsolvated hydroxy−benzenes[102,113,122,169−171] as did Kleinermann's group.[120,131,172−177] Recent findings for clusters of this type are summarized in the review of Ebata et al.[36] Therefore, the reader is referred to that article for further details and to the later section in this review summarizing the results for such cluster systems.

1. Substituted Benzenes Microsolvated by Water

In the following the IR/R2PI spectra of clusters of halogenated and methylated benzenes microsolvated by up to four water molecules will be compared with those of the analogous clusters with benzene. For methodical reasons, the qualitative structural assignments deduced for these clusters are first based exclusively on spectroscopic evidence. Subsequently, these assignments will be compared with the results—when available—from ab initio calculations of Tarakeshwar and Kim.[38,39] From these the cluster structures, binding energies and the type of the intermolecular bonds between the chromophore and the solvent moiety could be derived, which are partially summarized in Table 2.

To compare the IR/R2PI spectra of the clusters of substituted benzenes with those of benzene, the spectra of the $BZ{\cdot}W_{n=1-4}$ clusters have been remeasured under experimental conditions comparable to the spectra of the substituted benzenes.[178]

a. 1:1 Complexes. Figure 3 shows the IR/R2PI spectra of the 1:1 clusters of *p*-difluorobenzene (pDFB), fluorobenzene (FB), and benzene (BZ) with water. For comparison, the spectrum of anisole (ANI) with water is included. The 1:1 complexes of toluene (TO) and *p*-xylene (PX) with water could not be detected in the R2PI mass spectra, although they should exist. The R2PI bands assigned to the TO·W cluster by Bernstein et al.[179] could not be confirmed by means of IR/R2PI spectroscopy.

The spectra of the fluorinated benzenes with water, depicted in the first two traces in Figure 3, show two sharp bands very near the spectral positions of the symmetric ($\nu_1 = 3657$ cm^{-1}) and antisymmetric mode ($\nu_3 = 3756$ cm^{-1}) of water, marked by dotted lines. The band positions and their assignments are listed in Table 2. Compared with the spectrum of an isolated water molecule, three points stand out. First, both modes in the cluster show an equal red shift of 14 cm^{-1}. From the fact that in water both modes are linear combinations of two local, isoenergetic OH vibrations, a similar red shift of both normal modes indicates a similar binding interaction of both OH bonds. Second, the strong relative intensity of the ν_1 mode is surprising. While relative intensities in an IR/R2PI scan may not be relevant when transitions are saturated, the intensity ratio of both bands persists down to very low laser intensities. In isolated water, however, the ν_1 mode is about 1 order of magnitude less intense than the ν_3 mode. Thus, this intensity increase in the complex must be induced by the loss of symmetry due to the interaction with the chromophore. Third, the red shifts are practically equal for FB and pDFB. This equality suggests a local σ-type H-bond, preferably to a fluorine atom. If the water was bonded by a π-OH bond to the aromatic ring, differences in the shifts for FB and pDFB would be expected, if the electron-withdrawing effect for one fluorine alone is substantial.

The IR/R2PI spectrum of the corresponding cluster with benzene—third trace in Figure 3—is nearly identical to that first recorded and assigned by Pribble et al.[103,180] It is much more complicated than those just discussed and shows at least eight resolved transitions. They have been assigned to combination bands of large-amplitude motions which reflect the very floppy nature of this cluster. Although this spectrum is still lacking in its detailed characterization and assignment of the intermolecular vibrational structure,[25] the complex is meanwhile quite well characterized both experimentally and theoretically.

The first experimental study of its structure, supported by an ab initio calculation at the BSSE-

Table 2. Relevant Data of the Cluster Systems A·(water)$_n$ with A = *p*-Difluorobenzene (pDFB), Fluorobenzene (FB), Benzene (BZ), Toluene (TO), *p*-Xylene (PX), Anisole (ANI), Phenol (PH), *p*-Chlorofluorobenzene (pClFB) with *n* = 1−4: Structures, Relative Spectral Positions of the R2PI Fingerprint Bands Used for IR/R2PI, Theoretical Binding Energies, and Shifts of the OH Stretches of Water

cluster	structure	$\Delta\nu^a$ (cm^{-1})	$-\Delta E_0{}^b$ (kcal/mol)	shifts of the OH stretch frequency^c (cm^{-1})				ref
A·(H$_2$O)$_1$				ν_1		ν_3		
pDFB	σ-F	167	2.80	−14		−14		38, 43, 178
FB	σ-F	118	2.68	−15		−14		38, 178
BZ	π-OH	49	2.23	−23		−25		240
ANI	σ-OH	117		−66		−28		178
PH		−353		−7		−8		102
pClFB	σ-F	145		−12		−12		213
	σ-Cl	194		−21		−17		
A·(H$_2$O)$_2$				$\nu_{bD,\,fD}$	$\nu_{\sigma D'}$	$\nu_{\pi D'}$	$\nu_{fD'}$	
pDFB	σ-F	267	8.46 (5.01)	−54, −15	−65.5		−7	39, 178
FB	σ-F	182	8.24 (4.79)	−53, −14	−66.5		−7	39, 178
BZ	π-OH	75	7.17 (3.71)	−51, −27		−89.5	−23	180
TO	π-OH	33	8.44 (5.02)	−66, −24		−96.5	−24	178
PX	π-OH	−16		−69, −29		−106.5	−26	178
ANI	σ-OH	106		−65, −22	−197.5		−21	178
PH	cyclic	−121		−48, −13	−192.5		−20	102
A·(H$_2$O)$_3$				ν_{rD}	$\nu_{\pi D}$	ν_{fD}		
pDFB	π-OH	167	15.64 (3.65)	−93, −29.7	−34	−21, − 15		178
FB	π-OH	147	15.76 (3.85)	−95, −29.6	−53	−26, − 15		178
BZ	π-OH	98	14.51 (2.54)	−110, −25, 37	−69	−10, −6		180
TO	π-OH	122	15.59 (3.67)	−121, −19, 27	−79	−11, −6		178
PX	π-OH	103		−126, −23, 18	−89	−12, −8		178
ANI	π-OH	62		−139, −21, 29	−87	−16		178
PH	cyclic	−90		−188, −152, −82		−11, −7, −4		102
A·(H$_2$O)$_4$				ν_{rD}	$\nu_{\pi D}$	ν_{fD}		
PDFB	π-OH	167	26.09 (4.39)	−4	−30	−20, −5, 1		178
FB	π-OH	191	26.10 (4.39)	−73, 5	−53	−21, −1, 6		178
BZ	π-OH	100	24.61 (2.84)	−49, 11, 45	−62	−1, 10		180
TO	π-OH	108	25.84 (4.06)	−43, 14, 47	−71	−1, 7		178
PX	π-OH	63		−57, −6, 40	−91	−6, 4		178

[a] The $\Delta\nu$ values are the shifts of the 0_0^0 transitions in the complex relative to the ν_{00} of the bare chromophore. [b] The ΔE values, calculated by Tarakeshwar and Kim[38,39,184,241] at the MP2/6-31+G* level, are ZPVE-corrected binding energies with 50% BSSE correction. The energies inside the parentheses represent the binding energy of the water subcluster binding to the chromophore A, while those outside represent the binding energy of *n* water monomers to A. [c] The shifts are given relative to the values of free water (ν_1 = 3657 cm^{-1}, ν_3 = 3756 cm^{-1} [242]), the water dimer (ν_{bD} = 3601 cm^{-1}, ν_{fD} = 3735 cm^{-1}, $\nu_{fA'}$ = 3697.5 cm^{-1} (averaged value, see ref 178), $\nu_{fA'}$ = 3745 cm^{-1}), trimer (ν_{rD} = 3533 cm^{-1}, ν_{fD} = 3726 cm^{-1}), and tetramer (ν_r = 3416 cm^{-1}, ν_{fD} = 3714 cm^{-1}), respectively.[84]

corrected MP2/6-31G** level, were given by Suzuki et al.[137] From fully rotationally resolved spectra they could deduce a structure with a quasi-freely rotating water molecule, positioned above the benzene plane and with both hydrogen atoms pointing toward the π-cloud. In both the experimental and theoretical structure, water is situated nearly 1 Å within the vdW contacts of both subunits, which according to these authors is a clear manifestation of H-bond formation. The distance between the centers of mass of both moieties was determined to be 3.347 Å.

The current knowledge about this cluster from a number of recent theoretical investigations[181−184] indicates that the binding energy D_0 is in the range of 1.63−2.78 kcal/mol and that the potential well is extremely flat. Although the minimum energy structure can be considered to have only a single hydrogen bond, vibrational averaging renders the hydrogens indistinguishable. This prediction is in agreement with the experimental observation that the complex is a symmetric top. The lability of this complex is reflected in the large-amplitude motions of the water molecules above the aromatic ring. It was found that water may rotate freely around its C_2 *z*-axis whereas the motions around the perpendicular axes are more hindered. The motion around the *y*-axis, situated in the molecular plane of water, leads to a bending mode at about 260 cm^{-1} and around the *x*-axis to a so-called "swapping motion" at a frequency of about 47 cm^{-1}.[181]

In a recent ab initio study the binding energy and the type of interaction has been scrutinized more closely by Kim and collaborators using the MP2 (second-order Møller−Plesset perturbation theory) and SAPT (symmetry-adapted perturbation theory) methods and relatively large basis sets ranging from 6-31+G* to TZ2P++ and aug-cc-pVDZ. For a detailed account the reader is referred to the review article by these authors in this issue. With a zero-point vibrational energy correction (ZPVE) and a 50% compensation of the basis-set superposition error (BSSE) they obtained a binding energy ($-\Delta E_0$) of 2.86 ±1.13 kcal/mol, which compares nicely with the experimental value of 2.44 ± 0.09 kcal/mol.[185] Their SAPT analysis indicates that exchange repulsion plays a crucial role in this floppy complex and that the attractive forces are mainly of dispersive nature.

Comparing the simple IR/R2PI spectra for FB·W and pDFB·W with the complicated one of BZ·W, it is evident that the binding of water to the fluorinated chromophores drastically reduces the degrees of freedom for intermolecular motion. Thus, two nonequivalent intermolecular bonds between the water molecule and a FB or pDFB chromophore may be anticipated, with the fluorine substituent being in-

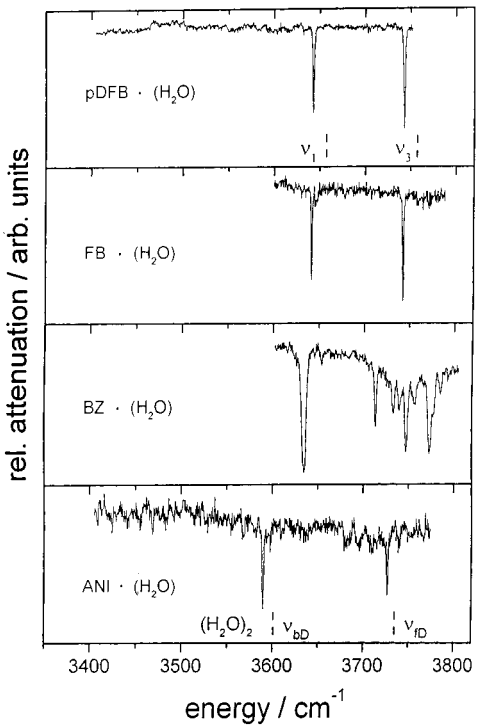

Figure 3. IR/R2PI spectra measured in the region of the OH stretches of water. The spectra were recorded with the R2PI laser fixed to the 0_0^0 transitions of the clusters A·(water) with A = pDFB, FB, BZ, ANI. The dashed lines represent the positions of the OH modes in isolated water (ν_1, ν_3) and those of the water donor molecule in the water dimer (ν_{bD}, ν_{fD}).

volved in one. Thus, a local σ-type H-bond should account for these simple spectra. Such a conclusion was originally not drawn, despite the similarity of the spectra for FB and pDFB. Guided by the thermodynamic behavior of fluorinated aromatics, as discussed below, Barth et al.[178] tentatively assigned a π-OH H-bonded structure for the 1:1 and, as will be seen later, also the 1:2 complexes similar to the corresponding complexes with benzene. They rationalized the reduced spectral complexity as compared to that with BZ to a more rigid structure induced by the local dipole moments of the C−F group(s).

Recently further experimental support for a local σ-type H-bonds to the halogen were provided by Reimann et al.[186] from the IR/R2PI spectra of the 1:1 clusters of *p*-chlorofluorobenzene (pCLFB) and chlorobenzene (CLB) with water. The R2PI spectrum of pCLFB·W contained several resonances (Table 2). From the IR/R2PI spectra measured for each UV transition, the existence of only two different isomers could be extracted. One exhibited a vibrational spectrum nearly identical to that of FB·W and the other a spectrum very similar to that of CLB·W. From these similarities one also may deduce a local, σ-type H-bond to the halogen substituent. In the alternative case of a π-OH H-bonded cluster, the shifts for the isomeric structures of pCLFB should be different from those of FB and CLB.

In the case of the ANI·W cluster, a structure with a classical σ-type O···HO hydrogen bond is expected, with the methoxy group acting as H-bond acceptor due to its very electronegative oxygen atom. The IR/R2PI spectrum recorded for this cluster (bottom trace Figure 3) shows two sharp bands, one positioned near the ν_3 stretch of water and the other strongly red shifted. The positions of both bands are very similar to that of the bound donor-OH and free-donor OH modes in the isolated water dimer, which are indicated by the dotted lines. Apart from this similarity the large difference in the red shifts of both bands clearly reveals a local σ-type O···HO H-bond with water as a donor.

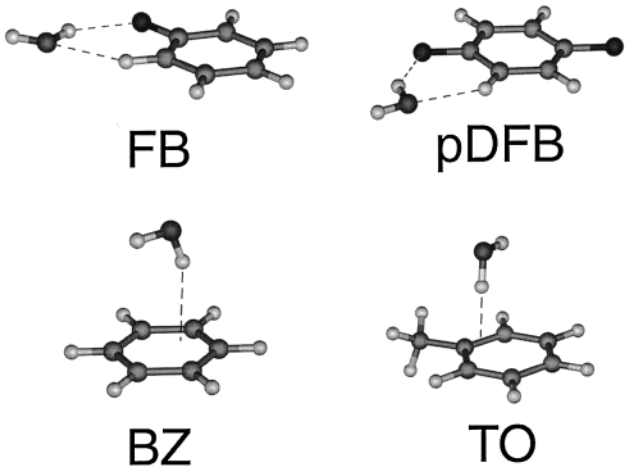

Figure 4. Minimum energy structures of the 1:1 clusters as calculated by Tarakeshwar and Kim at the MP2/6-31+G* level of theory.

The theoretically determined structures of the 1:1 clusters for pDFB, FB, BZ, and TO as calculated by Tarakeshwar and Kim[38,39,184] are depicted in Figure 4. For FB, pDFB, and BZ they correspond to the assignments deduced from the IR/R2PI spectra. Their ZPVE- and 50% BSSE-corrected binding energies $-\Delta E_0$, calculated for the electronic ground state are listed in Table 2. Originally the authors found two minimum energy structures for FB·W. One was a π-OH H-bonded isomer as in BZ·W, and one was a F··OH H-bonded one, termed σ-F isomer. In the latter the water was bound nearly in-plane by a H-bond to the fluorine and to a neighboring C−H group, forming a six-membered ring with the aromatic molecule. While further more refined ab initio calculations could not unambiguously decide which of the two isomers of FB·W is the global energy minimum, for pDFB·W, on the other hand, they found no such stable π-OH H-bonded structure. Instead, the only global energy minimum was an in-plane σ-F isomer similar to that calculated for FB·W. This exclusive stabilization of a σ-F isomer when going from FB to pDFB was rationalized by the increased reduction of the net charge in the π-system by the additive action of the two electron-withdrawing halogen substituents. In the calculated vibrational spectra, only the σ-F isomers of both 1:1 complexes exhibited nearly identical frequencies, as observed in the experimental spectra. Hence, Tarakeshwar et al.[38] also assigned a σ-isomer as a global energy minimum for both 1:1 clusters. This is an example where ab initio simulation alone was not yet able to predict the structure of such a weakly bonded complex unequivocally. As discussed above, several other properties of the spectra support such a σ-type H-bound structure.

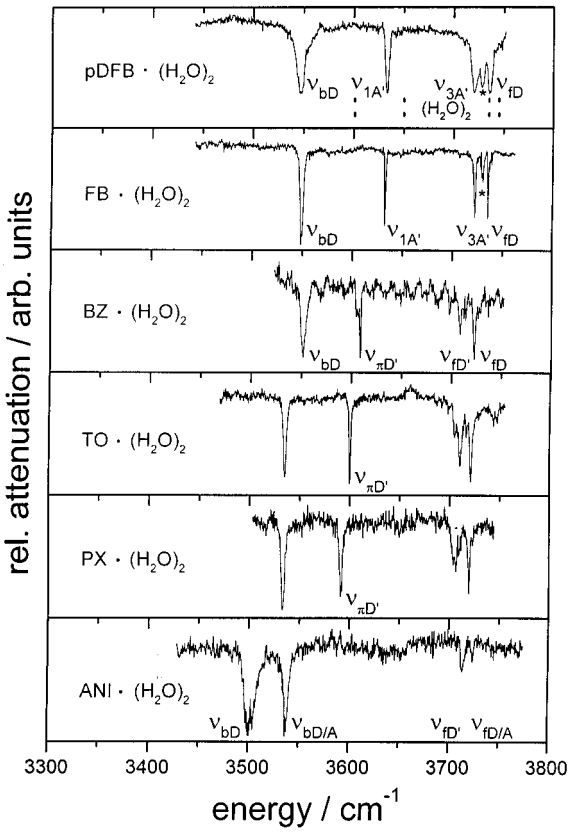

Figure 5. IR/R2PI spectra measured in the region of the OH stretches of water. The spectra were recorded with the R2PI laser fixed to the origin transitions of the clusters A·(water)$_2$ with A = pDFB, FB, BZ, TO, PX, ANI.

b. 1:2 Complexes. The IR/R2PI ion-depletion spectra of a water dimer attached to the chromophores pDFB, FB, BZ, TO, PX, and ANI, respectively, are depicted in descending order in Figure 5. For comparison, the positions of the vibrational bands of an isolated water dimer[79] are included in the first trace. The band positions and their assignments are summarized in Table 2. Apart from the spectra of ANI·W$_2$ at the bottom, the spectra are at first sight quite similar: On the blue side of the spectrum, very near to the ν_3 band of the water monomer, there are basically two bands which can be assigned to the ν_3 mode of a nearly unperturbed acceptor molecule in the water dimer and to the free donor OH mode (ν_{fD}). The strongly red-shifted band on the low-frequency side is assigned to the bound donor OH mode (ν_{bD}) and the less strongly red-shifted band near the ν_1 stretch of isolated water to the ν_1 mode of the acceptor. It should be pointed out that similar to the 1:1 complexes, the spectra from 1:2 clusters with FB and pDFB are basically identical. For the same reasons as discussed above, the assumption of a local H-bond to one fluorine substituent is compelling. The band marked by an asterisk is assigned to a combination band with a vdW mode.

In the spectrum of BZ·W$_2$ the large red shift of the previous (ν_1) acceptor mode (now marked as $\nu_{\pi D'}$) was attributed by Zwier et al.[103,149] to the formation of a relatively strong π-OH H-bond between the acceptor water and the π-electron system. It is red shifted relative to the corresponding band in the isolated water dimer by its donor function. This assignment was also supported by ab initio calculations. Therefore, the position of this band for π-OH-bonded complexes should be very sensitive to a changes in the electron density at the aromatic ring This is indeed observed: While the position of the donor OH mode (ν_{bD}) does not change much going from top to bottom in Figure 5, in the same order the position of the π-OH mode, marked as ($\nu_{\pi D'}$), shows an increasing red-shift going from BZ to PX. Taking for granted that in the case of the methylated benzenes a H-bonding site other than the π-system does not seem very plausible, the increase of the red-shift reflects a stronger π-OH H-bond with increasing net charge in the aromatic ring.

As in case of the 1:1 cluster series, the spectrum of ANI·W$_2$ (bottom trace in Figure 5) is very different from those of the fluorinated or methylated benzenes. Two bands appear around 3700 and 3500 cm^{-1}. While the latter are clearly bound donor (ν_{bD}) and bound donor/acceptor OH modes ($\nu_{bD/A}$), the former may be assigned to free donor OH modes (ν_{fD}) of the dangling OH groups. Thus, the spectra may be rationalized by a structure with the polar water dimer H-bonded to the oxygen of the methoxy group, which acts as a H-bond acceptor. For such a structure two strongly red-shifted donor modes are expected: one for the donor molecule and one for the acceptor molecule in the water dimer, with the latter forming a strong H-bond to the methoxy group. It must therefore be classified as a donor−acceptor molecule. For a donor−acceptor (D/A) a weaker red shift than for a pure donor is expected, because in the former the electron-donating and -accepting effects compensate each other to some degree. This order of red shifts for the stretches of both types of donor molecules was verified by Zwier et al. in ab initio calculations on free methanol clusters.[187] In summary, as for the ANI·W complex, the strong red shifts of the two donor modes in ANI·W$_2$ contrasts with the much weaker red shifts of the π-OH modes in the 1:2 clusters with BZ, TO, and PX or of the F···HO H-bonded donor modes in the clusters with FB and pDFB. If the red shift correlates with binding energy, an issue discussed separately in section III.B.1.e, this suggests a considerably weaker H-bond to the π-system as compared to an ordinary O···HO H-bond. This was also found in the ab initio calculation by Tarakeshwar and Kim and rationalized by a strong contribution from exchange repulsion in the π-OH "anchor" H-bond.

The results of the ab initio calculations for these 1:2 clusters are in excellent agreement with the above conclusions from the spectroscopic fingerprints. As depicted in Figure 6 , Tarakeshwar and Kim[38] found for FB·W$_2$ a global energy minimum for a structure with the water dimer σ-H-bonded to the fluorine and to an adjacent CH group of the aromatic ring, thus forming an eight-membered ring with the chromophore. According to their calculations, in the 1:2 cluster with BZ and TO the dimer is, on the other hand, bonded by a π-OH H-bond. At the MP2/6-31+G* level of theory, the binding energy $-\Delta E_0$ (see Table 1) of the dimer to FB and pDFB, respectively, is 4.79 and 5.01 kcal/mol. For comparison, the

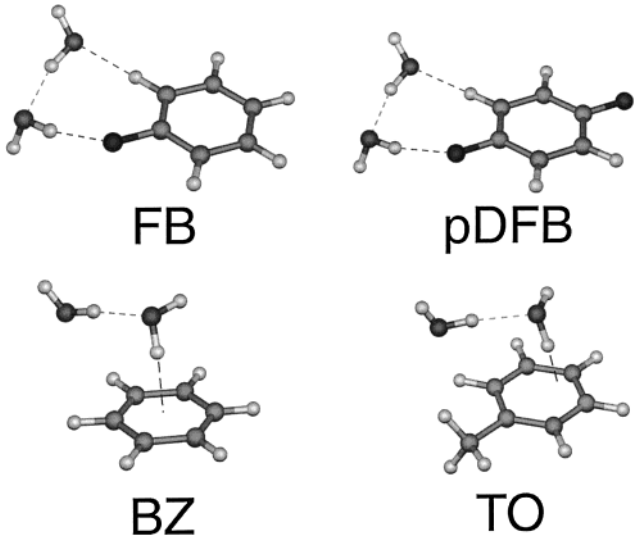

Figure 6. Minimum energy structures of the 1:2 clusters as calculated by Tarakeshwar and Kim at the MP2/6-31+G* level of theory.

calculated values of the π-OH H-bonded 1:2 complexes with BZ and TO were 3.71 and 5.02 kcal/mol, respectively. With the larger aug-cc-pVDZ basis set, the absolute energies of the π-OH-bonded 1:2 complexes increased (TO, 6.32 kcal/mol; BZ, 5.11 kcal/mol; FB, 4.76 kcal/mol; pDFB, 4.93 kcal/mol) but the relative energies within each group remained essentially the same.

c. 1:3 Complexes. The IR/R2PI spectra of 1:3 complexes with a water trimer attached to the same set of chromophores are depicted in Figure 7. The spectral positions and the assignments of the absorption bands are listed in Table 1. On the lower frequency side, a group of free donor OH vibrations appears, which is tightly bunched for pDFB and then splits for the other chromophores. A second group of three bound donor modes appears on the red side. Thus, the assumption of three more or less equivalent donor/acceptor molecules bonded into a ring with three dangling OH groups left suggests itself. However, the appearance of three well-separated donor absorptions for the trimer attached to a chromophore, as compared to one single donor mode observed for the isolated trimer,[79] should be pointed out. Obviously the low intensity modes in the isolated trimer gain intensity because of the loss of symmetry induced by the interaction with the aromatic ring. Particularly interesting is the development of this group going from top to bottom in Figure 7. While the splitting of the ring modes increases continuously from pDFB to PX, their more or less equal band intensities do not change much. On the red side next to the group of donor modes a band appears, which increasingly shifts to the red going from pDFB to PX. In the case of BZ, this band was assigned to the dangling OH group of a cyclic trimer forming an "anchor" π-OH H-bond, marked as $\nu_{\pi D'}$. It is similarly assigned in the spectra of TO and PX. The real new thing is that it should by similarly assigned in the spectra of FB and pDFB. The strongest evidence for such a π-OH H-bond between a water trimer and FB and pDFB are the different shifts of their vibrational bands.

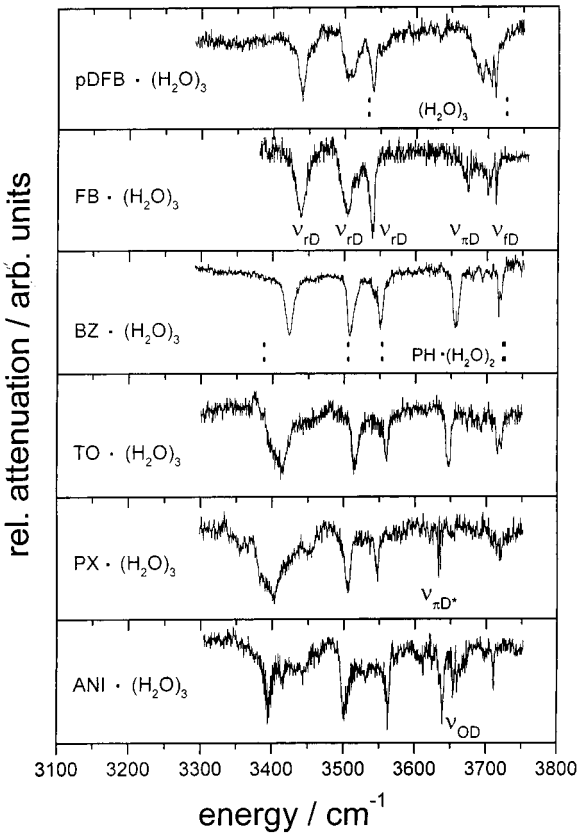

Figure 7. IR/R2PI spectra measured in the region of the OH stretches of water. The spectra were recorded with the R2PI laser fixed to the 0_0^0 transitions of the clusters A·W_3 with A = pDFB, FB, BZ, TO, PX, ANI. The dashed lines represent the spectral positions of the OH modes in W_3 (upper trace) and of PH·W_2 (middle trace).

Below the spectrum of BZ·W_3 the spectral positions of the vibrational bands recorded by Tanabe et al.[102] for PH·W_2 are included as dotted lines. Except for the missing band at the position of the $\nu_{\pi D'}$ band, the remaining bands have similar positions. Ebata et al.[188] assigned the three red-shifted bands to donor OH modes in a cyclic ring structure formed from the water dimer and the hydroxyl group of PH. A similar structure was calculated by Gerhards et al.[189] Hence, the assignment of a H-bonded ring of OH groups in the water trimer and the assignment of the $\nu_{\pi D'}$ mode is supported by this correspondence.

A surprising similarity is observed between the IR/R2PI spectrum of ANI·W_3 (bottom trace in Figure 5) and the other 1:3 complexes. From this one expects a common structure, irrespective of the substituents in the chromophores. Thus, a cyclic trimer bound both by dispersive forces and a π-OH anchor bond and a H···OH H-bond to the oxygen of the methoxy group is suggested from this vibrational fingerprint.

In summary, the local in-plane σ-type binding of water to the fluorine and the methoxy group substituent, as observed in the 1:1 and the 1:2 clusters, is gone in the 1:3 complexes in favor of a sandwich-type structure, where the cyclic water trimer should be mainly bound by a π-OH H-bond and the dispersive interaction with the π-system.

The conclusions on the structures of FB·W_3 and pDFB·W_3 is also confirmed by the ab initio calcula-

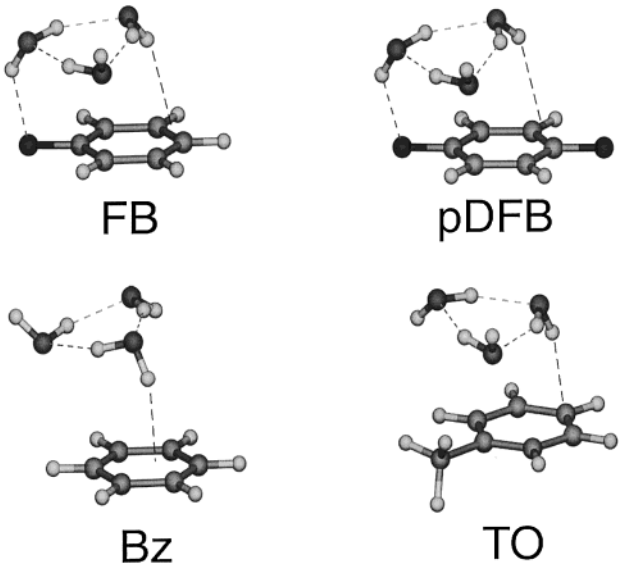

Figure 8. Minimum energy structures of the 1:3 clusters as calculated by Tarakeshwar and Kim at the MP2/6-31+G* level of theory.

tions. The theoretical structures for FB, pDFB, BZ, and TO are shown in Figure 8, and the binding energies are summarized in Table 1. Thus, in case of FB and pDFB, the σ-type local H-bonding switches to π-type H-bonding concomitant with a substantial increase of the dispersion energy by the stacking of both rings.

d. 1:4 Complexes. The IR/R2PI spectra of a water tetramer attached to the same set of chromophores are depicted in Figure 9. The relevant spectral data together with the assignments are summarized in Table 2. The spectra reveal a new feature: different from the spectra of the 1:2 and the 1:3 complexes, now three groups appear, each consisting of three vibrational bands. The first one, on the blue side, in the region of the free OH donor modes splits up into three modes, two of which are nearly isoenergetic for all substituents. Similar to the 1:3 complexes, the vibration assigned to the π-OH "anchor group" mode continuously shifts to the red going from FB to PX. The region of the red-shifted D/A ring OH modes contains two or three bands depending on the substituent. However, the band in the middle of this group seems to consist of two overlapping bands. As expected, the interaction with pDFB seems to be weakest, since the spectrum in that region resembles that of the highly symmetric free tetramer[79,140,190] more than in the case of the other chromophores. A third group, clearly visible for BZ, TO, and PX, is still further red shifted and appears in the region around 3200 cm^{-1}. It similarly contains three bands.

While the first two groups are assigned as before to free OH and ring OH modes, respectively, this third group is assigned to the first overtone transitions of the bending mode ν_2 of the water molecule. In the spectrum of BZ·W_4, recorded by Zwier, these bands, although weakly visible, were not assigned. Obviously they gain intensity by a Fermi resonance of the ν_2 mode with the strongly red-shifted ring modes. For comparison, below the trace of BZ·W_4 the positions of the OH modes of the PH·W_3 as measured

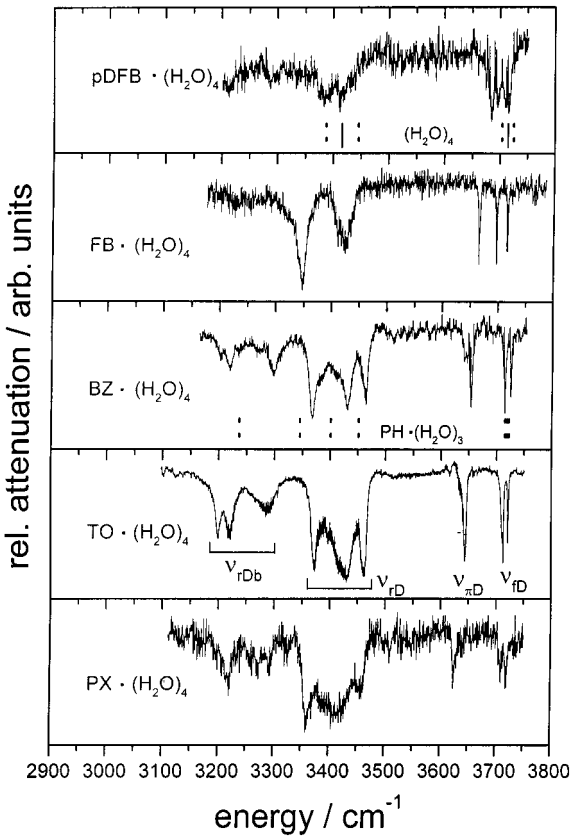

Figure 9. IR/R2PI spectra measured in the region of the OH stretches of water. The spectra were recorded with the R2PI laser fixed to the 0_0^0 transitions of the clusters A·W_4 with A = pDFB, FB, BZ, TO, PX. The spectral positions of the OH modes in W_4 (upper trace) and in PH·W_3 (middle trace) are denoted by dashed lines.

by Tanabe et al.[102] are included. Apart from a missing π-OH mode, the positions of the other bands look similar, again speaking for ring formation under inclusion of the hydroxyl group. The results of Tarakeshwar and Kim support the structural assignments for the 1:4 complexes of the substituted benzenes (see Figure 10 and Table 2). Again a "wetting" attachment of the subcluster is found for FB and pDFB, similar to the case of the 1:3 complex.

e. Summarizing Remarks. (1) With respect to the C−F···H hydrogen bond, it should be pointed out that it is very surprising and defies chemical experience. Fluorine incorporated into an organic molecule is known to be a poor H-bond acceptor. For example, the boiling point of many organic fluoro compounds with alcoholic groups differ only slightly from the corresponding hydrogenated compounds or are even lower than the latter. The question of H-bonding to covalently bound fluorine was also raised recently in the literature.[191−193] After a global search in the Cambridge and Brookhaven Protein Databanks, with thousands of structures analyzed, there were only two whose crystal structures contained fluorine as an acceptor. Thus, it seems that whenever other binding sites in an organic molecule compete with a fluorine atom for H-bonding in condensed phase, the bond to the latter is the least probable. Indeed, for the chromophore at a higher degree of microsolvation, the interaction with the aromatic ring and the

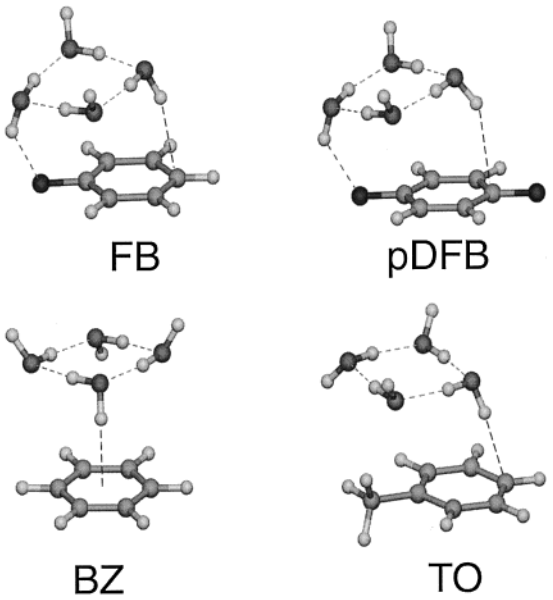

Figure 10. Minimum energy structures of the 1:4 clusters as calculated by Tarakeshwar and Kim at the MP2/6-31+G* level of theory.

intersolvent bonding becomes dominant. Recently Caminati et al.[194] studied the MW spectra of four isotopomers of the 1:1 clusters of difluoromethane and water. They assigned a structure where the molecule lies in the FCF plane of difluoromethane, linked through a O−H···F−C σ-type H-bond to one fluorine atom and opposite to the second. The study indicates that the geometry of this bond is considerably different from those of the O−H···O and O−H···N H-bonds, suggesting that the character of the lone pairs at fluorine is p rather than sp^3.

(2) A clear manifestation of the electron-withdrawing property of fluorine as a ring substituent is observable in the conformation of water bound to hexafluorobenzene. Danten et al.[195] calculated at the restricted Hartree−Fock and MP2 levels a structure in which the oxygen of water is situated above the aromatic ring and both hydrogen atoms are pointing away from it. Thus, water is bound inversely as in BZ·W. This unusual solute−solvent bond was rationalized by the cumulative depletion of the electronic ring charge induced by the six fluorine substituents. Thus, the lone-pair electrons of the oxygen of water are bound to the π-system in a Lewis acid−base type of interaction. A similar structure would be expected, for the adiabatic energy minimum of the ionized complexes A^+·W with A = BZ, FB, ClB, TO.

(3) For a qualitative discussion, the red shifts of the assigned π-OH stretches of $A{\cdot}W_{n=3\cdots4}$ are plotted in Figure 11 versus the net electron charge in the aromatic ring. The latter was obtained from ab initio energy optimization of the chromophore and a Mulliken population analysis.[178] For all chromophores with three and four water molecules, a linear dependence is observed. Thus, the red shift increases with increasing negative charge in the ring and decreases with the number of solvent molecules. This suggests the important role of electrostatic forces in the π-OH H-bond, which may diminish with decreasing polarity of the subcluster or increasing constraint by different

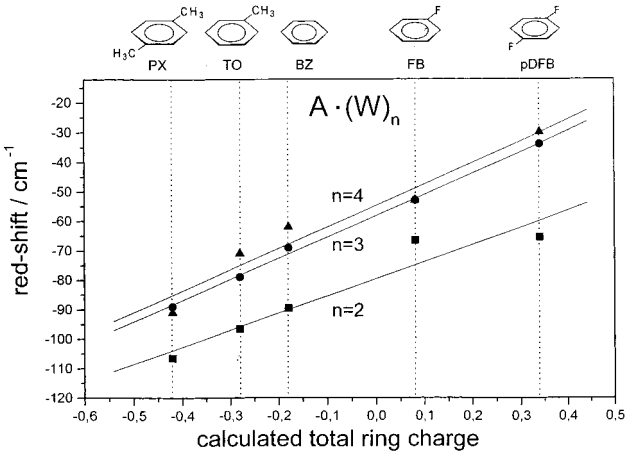

Figure 11. Red shifts of the assigned π-OH stretches of the clusters $A{\cdot}W_n$ plotted versus the net electron charges of the aromatic rings: A = BZ, TO, PX for $n = 2$ and A = pDFB, FB, BZ TO, PX for $n = 3$, 4. The red shifts of the stretches assigned to F··OH, σ-type H-bonded OH groups for $n = 2$ and A = pDFB, FB are included for comparison.

bonds. For the 1:2 clusters, both the shifts of the $\nu_{1A'}$ modes in the σ-F structures of FB and pDFB and of the $\nu_{\pi D}$ modes of the π-OH structures of BZ, TO, and PX are included. Thus, clear deviation from linearity is observed going from FB to pDFB. This behavior supports the earlier conclusion that for clusters larger than 1:2 a sandwich-type structure stabilized by π-OH bonding has to be assigned to all substituted benzenes studied. For the 1:2 clusters, linearity is only observed for the π-OH bonded clusters of BZ, TO, and PX. By decomposing of the binding energies of the 1:3 complexes, calculated at the MP2 level, Tarakeshwar et al.[247] found a linear correlation between the π-OH H-bonding induced red shift and the interaction energy between the chromophore and the π-OH bound water molecule.

(4) To give the reader a flavor of the excellent correspondence and accuracy of the harmonic vibrational frequencies derived from the ab initio calculations of Tarakeshwar and Kim, Figure 12 depicts the experimentally and theoretically derived spectra of the cluster system $FB{\cdot}W_n$ ($n = 1-4$). The calculated frequencies of the OH vibrations have been scaled exponentially with the vibrational energy.[196,197]

(5) The change in the binding at $n = 3$ for FB and pDFB may be viewed as a kind of "nonwetting−wetting" transition, as illustrated in Figure 13 for hydrated FB. Obviously for FB/pDFB the hydrophilic solvent is first bound to the polar sites at the rim of the aromatic ring before it starts in the 1:3 complex to cover the less hydrophilic part of the chromophore. One also could imagine from a comparison of these structures that the microsolvation in an early stage of the supersonic expansion takes place sequentially. This is also suggested from the anticipated much higher concentration of water monomers just behind the nozzle of a supersonic expansion as compared to that of larger water clusters.

(6) Tarakeshwar et al.[247] found for the 1:3 complexes with FB and pDFB in addition to the π-OH bond an additional σ-F H-bond, which was considerably weaker than in the 1:2 complexes. For all chromophores they calculated two isomeric structures

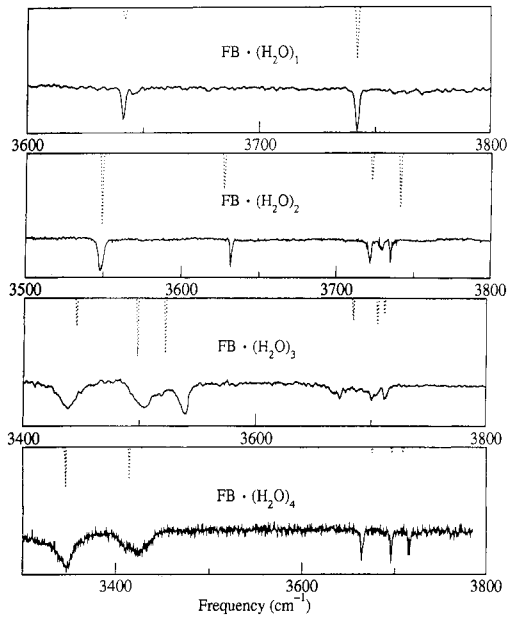

Figure 12. IR/R2PI vibrational spectra of FB·W$_{n=1-4}$ clusters together with the exponentially scaled vibrational spectra calculated by Tarakeshwar and Kim in harmonic approximation at the MP2/6-31+G* level of theory.

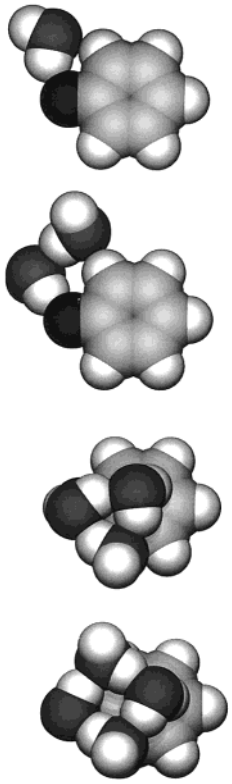

Figure 13. Minimum energy structures of the FB·W$_{n=1-4}$ clusters calculated by Tarakeshwar and Kim at the MP2/6-31+G* level of theory. For $n = 3$, a transition to π-OH H-bonding takes place.

of the 1:3 complex, differing mainly by the sense of hydrogen bonding in the water trimer, which can be clockwise and counter clockwise, respectively. The structures are isoenergetic but differ slightly in their vibrational spectra, in particular in the region of the ring OH modes. Both isomers are expected to transform easily into each other by flipping of the non bonding OH groups. This, and shorter predissociation lifetimes, should account for the anomaleous width of bands assigned to the ring OH modes. Similar isomers are calculated for the 1:4 complexes.

(7) In the same study it was found, that the ring mode with the highest frequency is associated mainly with the π H-bonded water, while that with the lowest one is mainly localized at the water molecule with no H-bond to the chromophore

(8) There is one additional point to address: the reaction behavior of the microhydrated fluorobenzenes in the ionic state. With FB[198] and pDFB[199] in the 1:4 complexes a rapid nucleophilic substitution reaction (S_N2) sets in, giving phenol$^+$ and fluorophenol$^+$, respectively, and HF as a leaving group. Although exothermic already in the 1:1 complex, this ion−molecule reaction is kinetically hindered and exhibits an activation barrier which depends on the number of solvent molecules. An earlier study of Martrenchard et al.[200] deduced a limit of $n \geq 3$.

In summary nearly all of the structural conclusions deduced from the IR/R2PI spectra of microhydrated substituted benzenes could be corroborated by the ab initio calculations of Tarakeshwar and Kim. From the excellent correspondence of experimental and theoretical vibrational spectra, the conclusions from an in depth theoretical analysis of the binding forces contributing to the minimum energy structures get particular persuasive power. For additional insights into the energetics and structure of these clusters, the reader is referred to the article of Kim et al. in this issue.

2. Substituted Benzene Microsolvated by Methanol

With methanol (MeOH) as the solvent, only one OH group is available per molecule. Thus, H-bonded, chainlike solvent subclusters have at most one free OH donor group available. In a cyclic subcluster, however, all free OH groups are engaged in the ring bonds and only dispersive and electrostatic forces are left for interaction with the chromophore. Thus, a sandwich-type structure bare of a π-OH "anchor" bond is expected for the 1:*n* clusters with a cyclic solvent subcluster.

In close spectral proximity to the OH mode, methanol possesses three CH stretching vibrations which may be interrogated as well for a H-bonding-induced frequency change. They may also serve as probes for the structure of the solvent moiety.

As will be seen, with methanol, different isomers for most of the 1:*n* cluster studied are formed in the supersonic expansion. Therefore, in the following discussion the cluster families of FB and pDFB are treated separately. The relevant data are enlisted in Table 3.

a. pDFB·(MeOH)$_n$ Complexes. Figure 14 summarizes the IR/R2PI ion-depletion spectra for the 1:*n* cluster system of pDFB microsolvated by up to three methanol molecules. The spectra have been recorded in the spectral region of the CH and OH stretches from 2800 to 3700 cm^{-1}. The upper trace depicts the spectrum of the 1:1 complex. In the higher frequency region the band of the ν_1 OH stretch of methanol appears, whereas the three CH stretches ν_2, ν_3, ν_9 are

Table 3. Relevant Data of the Cluster Systems: A·(MeOH)$_n$ with A = *p*-Difluorobenzene (pDFB), Fluorobenzene (FB), Benzene (BZ), Toluene (TO), *p*-Xylene (PX), *p*-Chlorofluorobenzene (pClFB), and Chlorobenzene (ClB) and *n* = 1−4: Structures, Relative Spectral Positions of the R2PI Fingerprint Bands Used for IR/R2PI, Theoretical Binding Energies, and Shifts of the OH and CH Stretches of the Methanol Molecules

					shift of the OH and CH stretch frequency[c] (cm^{-1})			
cluster	structure	$\Delta\nu$[a] (cm^{-1})	$-\Delta E_0$[b] (kcal/mol)		$\nu_{1(OH)}$	$\nu_{2(CH)}$	$\nu_{3(CH)}$	ref
				A·(MeOH)$_1$				
PDFB	σ-F	178	3.40		−17.2	−2.4	2.6	42
FB	σ-F	122	3.22		−19	−3.4	2.6	42, 43
BZ	π-OH	44	2.55		−43.5	−12.4	−7.9	42, 156
TO	π-OH	130			−48.3			199
PClFB	π-OH	69	2.45		−0.5	3.0	3.8	203
	σ-F	158	3.38		−17.5	−1.5	3.5	
	σ-Cl	186	2.45		−30.5	−2.5	0.9	
ClB	σ-Cl	139			−32.3	−5.0	0.9	203
				A·(MeOH)$_2$				
PDFB	σ-F	239.5		A	−37.4	3.6	18.6	42
				D	−83.2	−11.4	2.6	
FB	σ-F	159	10.47 (5.61)	A	−40.4	2.6	6.6	42
				D	−82.9	−12.9	−12.4	
	π-OH	141	10.14 (5.25)	A	−71.4	−0.4	2.6	
				D	−67.4	−14.4	−11.4	
BZ	π-OH	79		A	−79.1	−3.9	1.2	156
				D	−68.4	−16.8	−14.4	
TO	π-OH	105		A	−88.3	−5.0	−0.1	199
				D	−88.3	−17.5	13.9	
				A·(MeOH)$_3$				
PDFB	ring	111.5			5.6	−5.4	−5.4	42
					−8.8			
					−3.0			
	σ-F,chain	321.6		A	−18.8	−0.5	9.6	201
				D/A	−2.4			
				D	5.0	−12.4	−4.4	
FB	ring	90			7.6	−7.5	−3.4	42,43
					−11.8			
					−12.2			
	π-OH,chain	174		A	−65.9	3.6	5.6	42
				D/A	−0.3			
				D	−0.2	−12.4	−11.4	
BZ	π-OH,chain	147		A	−73.0	1.4	3.8	156
				D/A	3.0	−14.4	−10.4	
				D	0	−18.8	−20.4	
TO	π-OH,chain	153		A	−75.9	−1.5	4.0	199
				D/A	0.0	−13.0	−6.2	
				D	−16.2	−21.5	−19.5	

[a] The $\Delta\nu$ values are the shifts of the 0_0^0 transitions in the complex relative to the ν_{00} of the bare chromophore. [b] The ΔE values have been calculated by Tarakeshwar and Kim[201] at the MP2/6-31+G* in a similar way as in Table 2. The OH frequency shifts are given relative to the values of the methanol monomer (ν_1 = 3681.5 cm^{-1}),[243] the methanol dimer (ν_A = 3684.1 cm^{-1}, ν_D = 3574.4 cm^{-1}),[91] and the cyclic trimer (ν_{rD} = 3503.4 cm^{-1}, ν_{rD} = 3471.8 cm^{-1}, ν_{rD} = 3433.6 cm^{-1})[79] in the gas phase. The values for the chainlike trimer (ν_A = 3662 cm^{-1}, $\nu_{D/A}$ = 3433 cm^{-1}, ν_D = 3389 cm^{-1})[244] are taken from matrix investigations. The CH frequency shifts are related to the free methanol monomer (ν_2 = 2999.4 cm^{-1}, ν_3 = 2843.4 cm^{-1}),[245] because the CH frequencies of homogeneous methanol clusters are not known.

situated on the lower frequency side. The spectral positions of the corresponding bands in the isolated molecule are marked by dotted vertical lines. Additional bands appear on the blue side of the spectrum due to the aromatic CH vibrations ν_{20a}, ν_2, ν_{7b}, ν_{20b}. Their frequency change induced by microsolvation is marginal and nonsystematic. Hence, in the following they will not be discussed. From all vibrations recorded, the largest solvent-induced red shift is exhibited by the OH mode in this spectrum. From the small red shift of the ν_1 mode (−19 cm^{-1}), which is nearly equal to that in the FB·MeOH cluster (see Figure 16 and Table 2), a σ-type structure is assigned. This has also been found by ab initio simulation.[42] The corresponding structure is depicted in Figure 15.

The pattern changes for the 1:2 complex (Figure 16b). Now two OH bands appear, one with a weak and the other with a strong red shift, making the assignment of a H-bonded dimer beyond any doubt. The strongly red-shifted band originates from the bonded donor (ν_D) and the other from the acceptor (ν_A). The solvent's CH vibrations ν_2, ν_3, ν_9 also split into doublets, with the shifts considerably weaker than for the OH modes (see Table 2). The blue-shifted component of the CH band doublet is assigned to the acceptor (A) and the red-shifted component to the donor (D). This assignment takes into account that by transfer of electron density via a classical H-bond the bond of the hydrogen-donor group is weakened and its stretching frequency red shifted. This was also found recently in ab initio calculations on the structures of methanol clusters.[156]

As discussed for pDFB·W$_2$, the two fluorine substituents at the chromophore reduce the electron

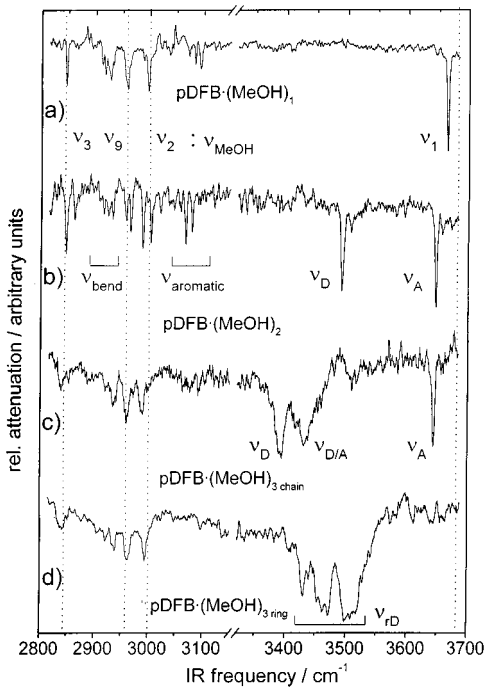

Figure 14. IR/R2PI spectra measured in the region of the OH and CH stretches of methanol. The spectra were recorded with the R2PI laser fixed to the 0_0^0 transitions of the clusters pDFB·(MeOH)$_n$ with (a) $n = 1$, (b) $n = 2$, (c) $n = 3$ with chainlike trimer, (d) $n = 3$ with ringlike trimer.

density of the π-system to such an extent that no π-bonded cluster structure (π-OH isomer) but only a σ-H bonded one (σ-F isomer) is found both by theory and experiment. Analogously, in the pDFB·M_2 complex, the ab initio calculations find the methanol dimer preferentially σ-type H-bonded to the fluorine and the neighboring CH group (see Figure 15).

In the R2PI spectrum of the 1:3 complex (not shown here), bands from two isomeric structures appear.[42] That of isomer I is blue shifted relative to the 0_0^0 transition of pDFB by 321 cm^{-1}, while that of isomer II it also blue shifted but only by 111 cm^{-1}. From these different shifts one anticipates a less polar methanol subcluster in isomer II and a more polar one in isomer I. Their IR/R2PI spectra are shown in the traces c and d in Figure 14. From the number of OH bands there is no doubt that in both isomers the subcluster is a methanol trimer. Isomer I (Figure 14c) exhibits a sharp, free OH acceptor mode (ν_A) and two broad, red-shifted donor modes. Thus, the fingerprint suggests a chainlike trimer subcluster. The band with the largest red shift is assigned to a bound donor OH (ν_D) and the less red-shifted one to the bound donor/acceptor OH ($\nu_{D/A}$). In the fingerprint spectrum of isomer II, depicted in Figure 14d, only three broad and similarly red-shifted donor modes appear, indicating a cyclic trimer. It should be noted that an isolated methanol trimer in its energetic ground state also exhibits a cyclic structure.[154] A comparison of the spectra measured for the isolated and associated cyclic methanol trimer reveals agreement within 10 cm^{-1}. This reflects the reduced interaction of the ring with the chromophore which should mainly be of dispersive nature.

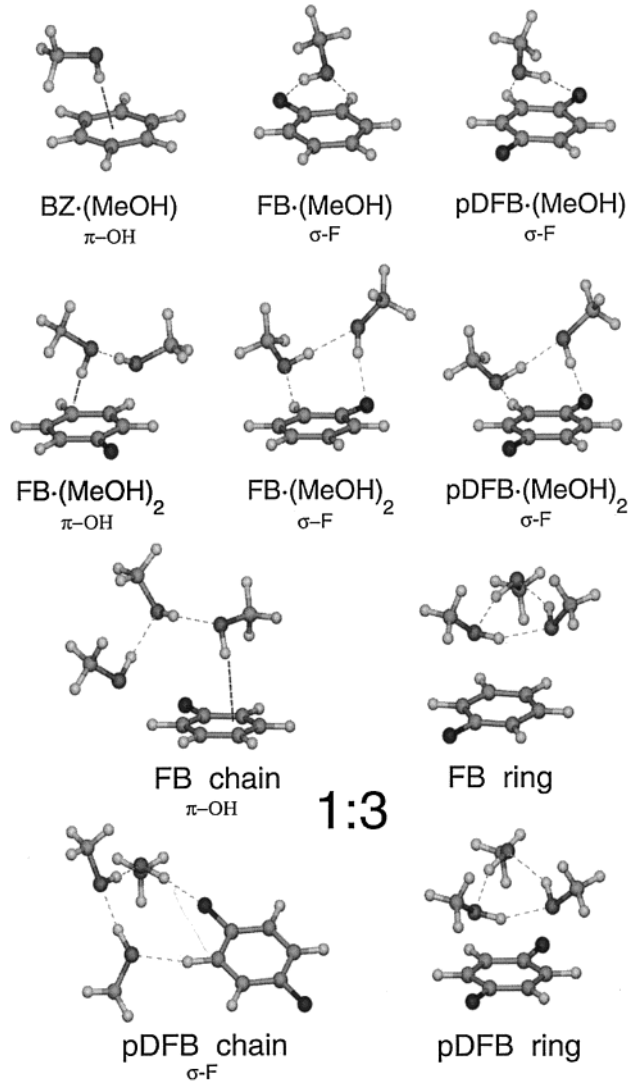

Figure 15. Minimum energy structures for 1:*n* clusters with methanol: 1:1 clusters with BZ, FB, pDFB; 1:2 clusters with FB (two isomers). All structures were calculated by Tarakeshwar and Kim at the MP2/6-31+G* level of theory. The structures of the 1:2 cluster with pDFB and of the 1:3 clusters with FB and pDFB are "artist view"-illustrations of the structures assigned from the vibrational spectra.

The CH vibrational bands exhibit a similar behavior as the OH bands: they are broad and unresolved for the cyclic isomer II, probably due to an overlap of three nearly equivalent donor CH stretches. In the linear isomer I they split up into two bands. One is relatively broad and intense, while the other, situated on the red-sided wing of the intense one, has a much smaller intensity and also looks narrower than the other.

The IR/R2PI spectrum of the 1:4 complex (not shown here) reveals only the signature of a ring-like structure for the tetramer.

Instead of analyzing the pDFB spectra further, the corresponding spectra for FB shall be briefly reviewed, since here the chromophore has an increased net charge in the π-system as compared to pDFB and therefore exhibits different binding sites for a subcluster.

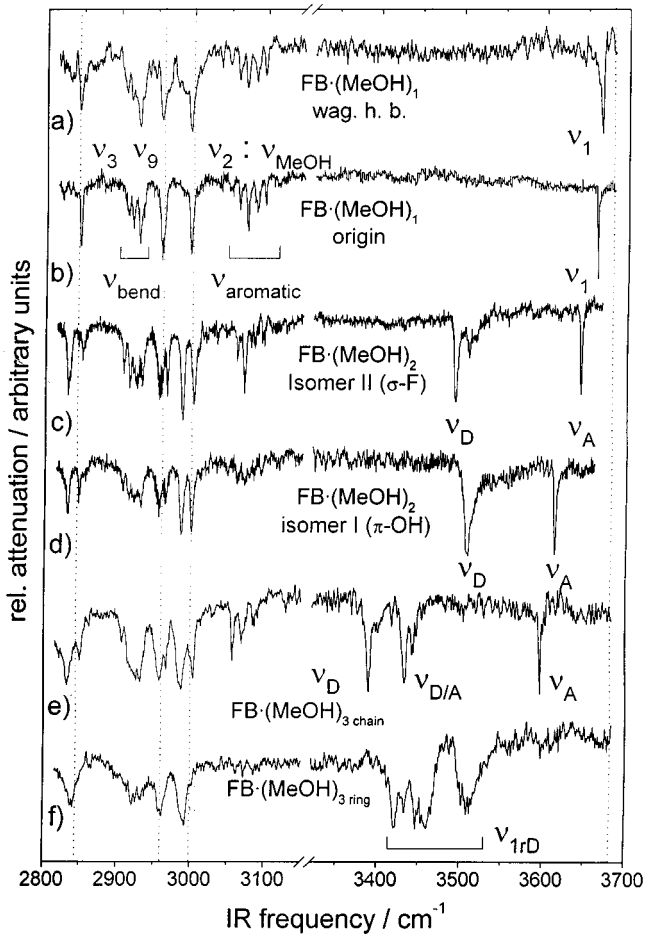

Figure 16. IR/R2PI spectra measured in the region of the OH and CH stretches of methanol. The spectra were recorded (except for a) with the R2PI laser fixed to the origin transitions of the clusters FB·$(MeOH)_n$ with (a) n = 1 sampled at a hot band (h.b.), (b) n = 1, (c) for n = 2 as σ-F bonded isomer II, (d) for n = 2 as π-OH bonded isomer I, (e) n = 3 with chainlike trimer, (f) n = 3 with ringlike trimer.

b. Fb·$(MeOH)_n$ Complexes. The earlier illustration of a typical series of R2PI spectra, depicted in Figure 2, summarizes the R2PI spectra of the product ions of a distribution of smaller FB·$(MeOH)_n$ ($n < 5$) clusters. The ionizing laser was scanned in the vicinity of the $S_1 \leftarrow S_0$ 0_0^0 transition. The bands in the R2PI spectra of nearly all product ions depicted are assigned by means of the IR/R2PI vibrational spectra to the neutral precursor cluster.

As discussed earlier, a direct assignment for most UV bands in these spectra is a priori not possible, since often several bands appear in an R2PI spectrum of one product ion, which can be assigned to (a) the origin of the cluster, (b) a hot band, (c) an intermolecular vibration in S_1, (d) an isomer, or (e) a larger cluster fragmenting into the same ionic channel. Although several of these possibilities can be checked by various procedures, among which UV/UV spectral hole-burning spectroscopy is the most promising one, the size and structure of the precursor remains in many cases not assignable. However, with IR/R2PI spectroscopy, nearly all of the more intense bands may be assigned unequivocally.

The corresponding IR/R2PI spectra recorded on the respective UV fingerprint bands are depicted in Figure 16. Traces a and b are sampled with the UV probe laser fixed to the bands 2 and 3, respectively, of the R2PI spectrum in Figure 2. Both spectra exhibit one OH stretch, with a slightly different shift. Hence, they do not originate from an identical ground-state cluster. Buchhold et al.[201] could rule out that they stem from different isomers. They could show that the vibrational spectrum depicted in trace a in Figure 16 is sampled from a hot band (hb) of the 1:1 complex (band 2 in Figure 2.) while that in trace b stems from the vibrational origin (band 3 in Figure 2.). In ab initio calculations, Tarakeshwar and Kim[201] found also only one minimum energy cluster structure where the methanol is H-bonded to the fluorine atom and to the ortho C−H group in a slightly out of plane configuration (σ-F isomer in Figure 15). Even at the very low temperature of the supersonic beam, which is estimated for small vibrations to be in the range from 10 to 20 K, it may still perform a wagging motion by interchanging the lobes of the lone pair orbitals of the oxygen donor. It should be pointed out that the reduced red shift of the OH mode of the wagging methanol molecule indicates a weakening of its F···HO H-bond. Tarakeshwar and Kim calculated at the MP2/6-31+G* level for a π-OH H-bonded isomer a binding energy of 2.96 kcal/mol and for the σ-bound isomer a value of 3.22 kcal/mol. Thus, the difference between both are within the computational uncertainty. However, since the experimental red shift of the OH mode of FB·MeOH is nearly equal to that of pDFB·MeOH, where a π-OH isomer is unstable, a σ-F isomer is the global energy minimum in both clusters. Interestingly, the binding energies for the analogous isomers of FB with water are only 1.86 and 2.68 kcal/mol, respectively (see Table 2). Thus, the H-bonds of methanol with FB are considerably stronger than those of water, i.e., 3.22 kcal/mol as compared to 2.68 kcal/mol. An analysis of the contributions of the different binding forces to the stabilization energy revealed a nearly 80% increase of the dispersion interaction for methanol, which is partially canceled by an increased exchange repulsion.[202]

Riehn et al.[203] recently observed three different isomers of *p*-chlorofluorobenzene·MeOH. Similarly to pClFB·W, two isomers exhibited nearly identical spectral shifts in the frequency of the OH mode as the 1:1 complexes with FB and ClB, respectively (see Table 2). From this similarity a σ-type local H-bond to a halogen may be deduced. In the third isomer of the 1:1 complex, methanol was bound to the chromophore by a π-OH H-bond. The corresponding isomer was not found for pClFBZ·W, as described above. This difference can also be rationalized by the stronger π-OH interaction of methanol with the aromatic ring as compared to water. The quantum calculation strongly supported these structural assignments by the magnitude and order of the calculated vibrational shifts. Interestingly, for the three isomers (σ-F, σ-Cl, π-OH), they calculated H-bonding-induced shifts of the OH stretches of (−8.6, −17.9,

2.5 cm^{-1}) which reproduce the experimental ones of (-17.5, -30.5, -0.5 cm^{-1}) astonishingly well. The corresponding intermolecular binding energies were (3.38, 2.45, 2.45 kcal/mol). Hence, although the binding energies of the σ-Cl and π-OH isomers are very similar, the shifts of the OH vibration differ considerably. Also, the σ-Cl isomer exhibits a twice as large red shift as the σ-F isomer while its binding energy amounts to only three-quarters of that of the σ_F isomer. From this one has to conclude that the absolute magnitude of a H-bond-induced frequency shift generally may not be correlated with the strength of a H-bond. However, for similar H-bonds, such a correlation seems reasonable.

Interestingly, the 1:2 cluster exists in two isomeric forms. The corresponding IR/R2PI spectra are depicted in Figure 16c,d. Both were sampled at the UV fingerprint bands 4 and 5, respectively, in the R2PI spectra in Figure 2b,c. Hence, both 1:2 clusters appear after R2PI in the two product ion channels FB^+·MeOH and $anisole^+$. While both IR/R2PI vibrational spectra clearly exhibit the signature of a H-bonded methanol dimer, it is also evident that each spectrum must be assigned to a different cluster structure. The one, named isomer I, exhibits a strongly red-shifted free acceptor mode (ν_A), whereas that of isomer II is only weakly red shifted. The spectrum of isomer I resembles that of the BZ·$(MeOH)_2$ complex, first recorded by Pribble et al.[139] and assigned by them to a π-OH-bonded dimer (see Table 3). Thus, isomer I should have a similar structure. On the other hand, the spectrum of isomer II is very similar to that of the pDFB·$(MeOH)_2$ complex (Figure 14), assigned to a σ-F isomer. Hence, a similar structure is assigned to isomer II. These different isomers have also been found in ab initio calculations by Tarakeshwar and Kim and are depicted in Figure 15.

The 1:3 complex also exists in two isomeric structures. From the recorded IR/2PI spectra in Figure 16e,f, a linear and a cyclic methanol trimer may be deduced. Therefore, the isomers of the 1:3 cluster of FB and pDFB at first sight look similar. However, from the much stronger red shift of the acceptor OH band of the linear trimer in the complex with FB as compared to that with pDFB, different binding sites of the "anchor" H-bond at the aromatic ring may be inferred. With FB the trimer is bound to the π-system, while with pDFB it binds to the fluorine substituent.[42] This again underpins the higher charge density in the aromatic ring of FB as compared to that of pDFB.

Closing the discussion of this cluster system it should be pointed out that the nucleophilic substitution reaction, taking place in FB^+·$(MeOH)_n$ for $n = 2$, is quantitative for both isomeric structures of the 1:3 complex. This can be seen in Figure 2, where the fingerprints of the neutral 1:3 precursors exclusively appear in the $anisole^+$ product ion channel. Thus, it may be assumed that the microsolvation in the ionized complex is reorganized in less than nanoseconds, giving a transition state for the reaction which is independent from the structure of the neutral precursor.

Summarizing these results for the fluorinated benzenes microsolvated by methanol, the following conclusions may be drawn. (1) In the 1:1 complex of both fluorinated benzenes, methanol is bonded planar to the aromatic ring via a local F···OH and O···HC σ-type H-bond. This binding behavior is analogous to that with water. (2) In the case of the much more polar methanol dimer, FB offers two binding sites, i.e., the π-electron system and the fluorine substituent. While with the water dimer the in-plane σ-H-bonded structure is the most stable one, with methanol the stabilization energies of the π-OH and the σ-F isomers are similar. In pDFB, however, only the σ-type bonding is observed. (3) The methanol trimer may be attached to the fluorinated benzenes in linear or cyclic form. To benzene or toluene, on the other hand, only linear trimers are attached. In clusters with FB and, in particular, pDFB, the strength of the π-OH "anchor" bond for the linear trimer is weakened due the charge-withdrawing effect of the substituents. With both chromophores the dispersively bound cyclic trimer then competes with the H-bound linear form. Thus, the three O···HO H-bonds in the strained cyclic methanol trimer should provide a similar amount of binding energy, as two linear O···HO H-bonds plus one π-OH H-bond. (4) The reduction in electron density of the π-system caused by the fluorine substituent is also underlined by the different binding sites of the chainlike trimer. In FB, the π-system provides a stronger binding for the highly polar linear trimer than does the fluorine substituent. With pDFB, however, this binding site is less favorable due to the cumulative substituent effect. In this case a fluorine atom is the only binding site. (5) Even hot bands may be distinguished from cold bands by means of different IR vibrational bands. (6) The absolute red shift of the stretches of H-bonds going to different bonding sites do not correlate with the binding energies, as calculated by high-level ab initio calculations. The results demonstrate that IR/R2PI spectra, recorded in the region of the OH stretches, contain crucial information on the structure of a microsolvation environment and that the intramolecular H-bonding controls both the conformational structure and the relative conformational abundance. (7) The assignments and conclusions deduced from the observed OH transitions have been corroborated or even predicted for most of the 1:n clusters ($n < 4$), as discussed above, by ab initio calculations by Tarakeshwar and Kim. The harmonic vibrations calculated from their minimum energy structures nicely reflect the main features deduced from the experimental spectra. That there are still some discrepancies between experiment and theory is necessarily caused by the finite size of the basis sets and by the harmonic approximation employed for calculating the vibrational modes. As pointed out recently, the error in the theoretical frequencies calculated within the harmonic approximation may be quite substantial.[204] An earlier study by Brenner et al.[205] on the system pDFB·$W_{n=1-3}$, using a semiempirical perturbation exchange model, calculated both similar and very different structures and, in particular, more stable isomers for $n = 2$, 3 than observed.

In contrast, the simulations with MP2 and reasonably large basis sets always provided the same number of structural isomers as those found in the IR/R2PI spectra, except for the 1:1 complexes with FB. This good agreement was not the case for the DFT-B3LYP simulations, which had been conducted in most cases parallel to MP2. (8) The results presented above, illustrate the different types of H-bonds in a microsolvated substituted benzene cluster, i.e., both those in the solvent moiety and those between the latter and the aromatic chromophore. The strongest solute−solvent interaction is mostly a π-OH H-bond, the strength of which is altered by the +I or −I charge shifting effect of the substituent. By comparing the vibrational spectra for different substituents and different number of molecules, they could be read in an inductive way like fingerprints, which are changing in a characteristic way within a family of clusters. Although no detailed structure could be derived nor the quantitative energetics be deduced by this correlation, the main feature of the structure could be determined unambiguously. These spectroscopic assignments have been refined for several clusters by state of the art, high-level ab initio calculations, which gave both minimum energy structures, isomers, binding energies, and "docking" sites together with the vibrational spectra in the harmonic approximation. The latter could be compared with the experimental vibrational spectra, thus allowing a verification of the assignment and of the calculated structures. It should be pointed out that neither spectroscopy nor theory alone would be sufficient for a convincing structural analysis.

C. Benzene and Substituted Benzenes Interacting with Chloro- and Fluoroform

Correlations between the structure of a molecule and a spectroscopic property depending on it are the rationales of many spectroscopic rules. The structural assignments made in the section above have been made in this very spirit. For the establishment of such rules, molecular probes with well-known spectral properties have been used.

In the past, the red shift of the CD stretch of deuteriochloroform served to evaluate the molecular basicity in series where H-bond formation was the dominant intermolecular interaction.[95] Nevertheless, the number of examples exhibiting an "unusual" shift was constantly increasing over the years. Examples are blue-shifted CH/CD stretches of h_1/d_1-chloroform[206] when acting as proton donor. Barnes and coworkers[207] recently measured a blue-shifted stretch for chloroform and bromoform induced by H-bonding to proton acceptors with dipolar groups such as carboxy, nitro, and sulfo compounds. The shift of the haloforms was in the range from +3 to +8 cm^{-1}. From MNDO calculations they rationalized this reversal of the shift by a rehybridization of the CH bond with a concomitant strengthening of its s-character, induced by a molecular distortion resulting from the intermolecular interaction.

Evidence of an analogous blue shift in the C−H vibration of a haloform molecule attached by a CH$\cdots\pi$-type H-bond to an aromatic molecule was lacking both in theory and experiment until recently. However, the existence of such a H-bonding interaction was supported by many experimental results.[208,209] For example, Reeves and Schneider[210] examined the association of chloroform with aromatic and olefinic solvents by ^{1}H NMR spectroscopy. The ^{1}H signal of chloroform shifted significantly upfield in benzene, toluene, or mesithylene, from which a specific interaction between chloroform and the aromatic substrate was deduced. This shift led to the conclusion that the hydrogen atom is situated, on average, above the plane of the aromatic ring forming a H-bond.

It required high-level ab initio calculations for a theoretically convincing treatment of this anomalous but relatively small blue shift in the vibration of a CH donor group involved in similar H-bonds. Hobza et al.[40] were the first to find by ab initio theory that molecules with carbon proton donors, such as methane, chloroform, or benzene, exhibit such a blue shift in the frequency of the CH stretch when bound to a π-electron system. Concomitant to the blue shift they identified a contraction, i.e., a strengthening of the CH bond. Since this behavior is opposite to the red shift observed for classical donor groups as discussed above, they coined the term "anti-hydrogen bond" for this anomalous interaction.

First experimental evidence of this effect was provided recently in the author's group for 1:1 clusters of chloroform (Cf) with benzene or fluorobenzene.[211] As an illustration, in Figure 17a the R2PI spectrum of the BZ·Cf cluster is depicted. A clear resonance is observed for this cluster, blue shifted by 178 cm^{-1} relative to the $S_1 \leftarrow S_0$ 6_0^1 transition in isolated benzene. The corresponding IR/R2PI spectrum in the region of the CH stretches was recorded at this cluster transition. The vibrational spectrum (Figure 17b) exhibits three absorption bands. For their assignment four different vibrational transitions come into question: the CH stretch of Cf (ν_{Cf}) and three CH vibrational transitions of benzene (ν_{20}) (ν_1 ν_6 ν_{19})(ν_8 ν_{19}). Only by using fully deuterated benzene (BZ(d_6)) could the CH mode of chloroform be isolated from the aromatic modes (Figure 17c)). It is blue shifted relative to its value in uncomplexed Cf by 14 cm^{-1} and overlaps with the vibrational mode ν_{20} of BZ(h_6). From ab initio calculations on this cluster, Hobza et al.[211] found one minimum structure with the Cf pointing with its CH bond to the π-system, very similar to a π-OH H-bond. Their anharmonic, counterpoise (cp)-BSSE-corrected calculations at the MP2/6-31G*-level of theory gave a blue shift for the CH vibration of 12 cm^{-1}. Later Cubero et al.[212] tried to differentiate between a hydrogen and an anti-hydrogen bond by a comparative analysis based on the electron density topology of these bonds and the Popelier criteria for H-bonds. However, no distinction between both types of bonds was achieved.

In a further experimental attempt to understand the molecular roots of this improper, blue-shifting H-bond, Reimann et al.[213] studied the CH shifts of both chloro- and fluoroform (Ff) attached to different substituted benzenes. Surprisingly the blue shift was

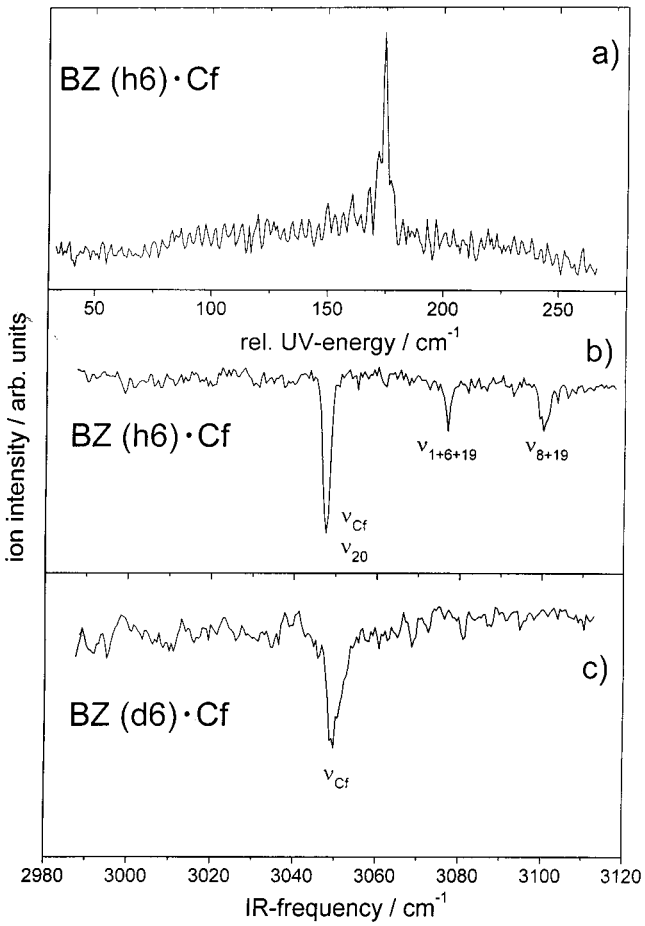

Figure 17. (a) R2PI spectrum measured for BZ^+·Cf in the vicinity of the $S_1 \leftarrow S_0$ 6_0^1 transition of BZ and IR/R2PI spectra measured in the region of the CH stretch of Cf and the CH stretches of BZ (b) for BZ (h6) and (c) BZ(d6).

Table 4

cluster	structure	$\Delta\nu^a$ (cm^{-1})	$-\Delta E_0$ (kcal/mol)	shift of the CH stretch frequency^b (cm^{-1})	ref
A·Cf				ν_1	
FB	π-CH	115	3.1^c	14	211
BZ	π-CH	178	3.2^d	14	211
TO	π-CH	188		13	213
A·Ff				ν_1	
FB	π-CH	220	2.2^c	21.5	214
BZ	π-CH	242		24	214
TO	π-CH	270		23	213
PX	π-CH	390		21	213

^{a} The $\Delta\nu$ values are the shifts of the 0_0^0 transitions in the complex relative to the ν_{00} of the bare chromophore. ^{b} The shifts are given relative to the values of free chloroform ($\nu_1 = 3033\ cm^{-1}$)[242] and fluoroform ($\nu_1 = 3035\ cm^{-1}$),[246] respectively. ^{c} ΔE values calculated by Havlas and Hobza[211] at the MP2/6-31G* level on CP-corrected PES. ^{d} BSSE-corrected ΔE value, calculated by Hobza and Spirko[40] at the MP2/6-31G* level.

only very weakly dependent on the substituent but significantly increased from Cf to Ff. As summarized in Table 4, for Ff the recorded shifts were between 20 and 25 cm^{-1} while for Cf the blue shifts were generally smaller than 15 cm^{-1}. For a sandwich-type FB·Ff complex, Hobza and co-workers calculated a value of 31 cm^{-1} within the harmonic approximation, which reduced to 21 cm^{-1} upon taking into account anharmonicity. This nearly perfectly agrees with the experimental result. The blue shift obviously increases with the electronegativity of the substituents at the CH donor group.

Since the term "anti-hydrogen bond" had aroused some debates and led to misunderstandings, Hobza et al. later proposed the term "improper, blue-shifting H-bond". As found theoretically, the red shift of the vibrational frequency induced in the X−H group of a classical H-bond donor is mainly due to a charge transfer from the acceptor into the antibonding orbital of the donor. By this the bond is relaxed, leading to a red shift. The blue shift, on the other hand, induced by an improper H-bond, cannot originate in a similar manner from a CT to the CH group. Hobza et al.[214] deduced from an analysis of the occupancy of the MOs that the anomalous vibrational shift is mainly due to a change in the conformation of the haloform induced by an electron transfer from the acceptor (π-system) into different molecular orbitals of the hydrogen-donor molecule. It is further traced back to a conformational change of the latter, which is induced by an anomalous electron transfer caused by H-bonding. For further details of the interpretation of this effect, the reader is referred to the article of Hobza et al. in this issue.

D. Literature Survey on Related Cluster Systems

In the following a short overview of additional findings on the microsolvation structure of substituted benzenes shall be given, without pretending completeness. In these examples the substituents are for the most part classical H-bond donors or acceptors such as the hydroxyl or amino substituents. Hence, the microsolvation structures are often dominated by these donor or acceptor sites.

Aniline (AN) as a chromophore has been studied mainly in Takeo's group. In the IR/R2PI vibrational spectrum of AN·ammonia,[111] the symmetric and antisymmetric stretches of the NH_2 group exhibited red shifts of −68 and −29 cm^{-1}, respectively, relative to the stretches of the uncomplexed chromophore. The decrease of the frequency difference between both stretches was rationalized by a classical NH···N H-bond between ammonia and a single NH group of AN as donor. By this bond the equivalence of the two NH bonds is broken, causing an increased frequency difference between both modes. A similar effect is observed in PH·W,[102,107] while in contrast to this, nearly equal shifts are observed for the OH modes in FB·W[198] (see Figure 3 first trace). For the latter a structure was assigned with both OH groups of water forming a σ-type H-bond of similar strength to the aromatic ring.[38] Nakanaga et al. also measured the depletion spectrum of the ionized complex AN^+·ammonia by R2PI/IR and observed only one strong absorption band at 3419 cm^{-1}. The latter was assigned to the free NH donor mode in the cation. The missing bound donor NH mode was assumed to lie at wavelengths outside of the working range of their IR source, i.e., at energies below 3200 cm^{-1}. From this interpretation they deduced a large increase of the strength of the H-bond in the ionized as compared to the neutral molecule. The IR/R2PI

spectrum of aniline dimer, taken in the region of the NH stretches, revealed a head-to-tail sandwich geometry with mutual NH···π H-bonds between the stacked molecules.[215] A similar face-to-face geometry with H-bond interaction was also deduced for AN·BZ, while in AN·cyclohexane (cH), no direct interaction between cH and the amino hydrogens could be found.[216] AN·pyrrole[217] also exhibited a NH···π-type H-bond, while for AN·Furan,[218] AN·dimethyl ether, and AN·triethylamine a NH-donor σ-type H-bond was deduced. In all these cases the assignments were supported by ab initio theory at various levels (UHF/6-31G**, MP2/4-31G**). The same group also studied the IR depletion spectra of the ionized complexes aniline$^+$·B with B = Ar, CO, water, ammonia, aniline, BZ, furan, pyrrole.[110,219] The bandwidth of the vibrational modes were much larger than those observed in the neutral complexes. This was attributed to the internal vibrational relaxation of the ionized chromophore into the intermolecular vibrational modes. Also, a linear relationship was found between the red shift of the free donor NH mode (ν_{free}) and the proton affinity of B. Since no clear physical meaning could be attributed to this relationship, it was rationalized as an indirect effect of the NH group involved in a strong H-bond.

A special type of chromophore is indole (IN), a fused heterocyclic system with an N−H group at the pyrrole ring. Although not a substituted benzene, results on its microhydration structure should be referred to because it exhibits several new and interesting aspects. In addition, it is the chromophore of the amino acid tryptophan, which has long be exploited as a fluorescence probe of the local structure and dynamics of proteins. The IN·$W_{n=1,2}$ clusters have been studied by Carney et al.[220] with IR/R2PI spectroscopy. For the 1:1 cluster, evidence of a NH···OH_2 σ-type H-bond could be given. Helm et al.[127] deduced for this cluster from highly resolved R2PI spectra with rotational fine structure a planar configuration. The best agreement between simulation and experiment was found when the oxygen atom of the water molecule is located 2.93 Å away from the hydrogen of the NH group of indole. This distance was later corrected by Kortner et al.,[221] who calculated from the rotational constants for the quasi-linear σ-type H-bond a heavy-atom separation of 3.07 Å and found indication of large-amplitude motions of water. This cluster was also one of the few cases where MATI resonances were observed.[128] For the 1:2 complex, Carney et al. deduced both experimentally and theoretically a structure with the water dimer forming a H-bonded bridge between the N−H and the π-phenyl ring of indole. The authors suggested that the formation of H-bonded bridges between different H-bonding sites on larger solute molecules may be a common feature of larger microhydrated molecules. The role of such bridges on proton and electron transfer was estimated to be an interesting issue for future studies. The same group[222] also investigated microhydrated 1- and 3-methylindole (1MIN/3MIN). From the IR/R2PI spectra, supported by ab initio calculations on the DFT B3LYP/ 6-31+G* level, they concluded that water is π-OH bonded to the phenyl ring both as single molecule, as dimer, and as cyclic trimer. Although DFT is not a good method to account for H-bonds with the aromatic π-system (see the contribution of Tarakeshwar et al. in this issue), these results are expected from intuition. The preference of π···OH instead of a NH···O σ-type H-bond could be caused by the electron-donating action of the methyl group. Interestingly, the 1:3 complex exhibited two isomers with different UV fingerprint bands. They differ in the orientation of the H-bonds in the water trimer ring relative to 1MIN (clockwise and counterclockwise). Thus, under supersonic cooling conditions, two chiral diastereomeric structures of the cyclic water trimers are bound to the chromophore.

Benzonitrile (BN) microsolvated by polar solvent molecules was also investigated recently. Part of the interest dedicated to this chromophore stems from its photophysical behavior in the S_1 state. Mordzinski et al.[223] reported dual fluorescence for the monomer, which they assigned to a charge-transfer (CT) reaction in the first electronically excited state. The structure of BN·W was investigated by Kobayashi et al.[224] with LIF spectroscopy, from which a planar structure of the cluster was deduced. Recently Helm et al.[225] investigated its structure with microwave and highly resolved optical spectroscopy. From the rotational constants of the complex, they assigned a cluster structure with the water molecule bound sidewise and in-plane to the aromatic ring by two H-bonds: one a π-type H-bond to the CN group and one a σ-type H-bond to the CH group in ortho position. The clusters BN·$W_{n=1-3}$ and BN·$(MeOH)_{n=1-3}$ have been studied with fluorescence-detected Raman and IR spectroscopy by Mikamis group.[108] The CC (ν_{12}), CN (ν_{CN}), CH (ν_{CH}), and OH stretches (ν_{OH}) have been examined for each species. Characteristic shifts were observed only for the CN (ν_{CN}) and OH stretches (ν_{OH}) involved in the bonding of the solvent subcluster to the chromophore. With the help of ab initio calculations at the HF/SCF 6-31G(d,p) level, they assigned the spectra to cluster structures, in which linear subclusters of W_n or $(MeOH)_n$ are H-bonded to both to the CN group and to the CH group in ortho position, forming in-plane rings with the aromatic molecule. For $n = 1$, very similar to the structure proposed by Helm et al., one donating OH group of water is H-bonded perpendicularly to the CN triple bond (π-type H-bond) with a concomitant red shift of the ν_{CN} mode. This is presumably due to geometrical constraints. In larger clusters with $n = 2$, 3, the binding site is exclusively the nitrogen (σ-type H-bonding), revealed by a blue shift of the ν_{CN} mode. Thus, π-bonding causes a weakening of the CN bond, while σ-type H-bonding increases the bond strength. With larger, more polar chains, the polar cyano group is obviously the preferred binding site. An analogous binding behavior was observed with methanol. With the FB·W_n clusters, such in-plane geometries were only observed for the 1:1 and 1:2 complexes, as discussed above.

Clusters consisting of phenol or one of its derivatives with water, methanol, ethanol, ammonia, and amines, etc., have been intensively studied by several groups. Phenol is the fundamental aromatic alcohol

and takes part in H-bonding networks with polar, protic solvent subclusters easily by virtue of its hydroxyl group, as discussed earlier.

A recent review of Ebata et al.[36] describes most of the results published until 1998 on microsolvated hydroxybenzenes, with particular consideration for the chromophores phenol (PH) and tropolone, together with a discussion of the IR spectroscopy of $PH_{n=2,3}$ clusters. Part of these results have also been included in Zwier's review articles.[25,226]

Early studies on such systems have been done by several groups.[169] The first size-specific study of clusters of the type PH·B with B = polar and nonpolar molecules was reported by Felker and coworkers.[107] They applied the IDSRS method (ionization-detected stimulated Raman spectroscopy) described in section II.B.4 and found that the phenolic CO and OH stretch fundamentals are more efficiently shifted by the hydrogen bonding than the other modes in the complex. Mikami and co-workers studied the structure of size-selected $PH{\cdot}W_{n=1-4}$ clusters in the S_0, S_1, and ionic state of PH.[102,106,168,188,227] The methods used were IR/R2PI, for which they used the acronym IDIRS (ionization-detected IR spectroscopy), fluorescence-detected IR spectroscopy (FDIRS), and trapped-ion IR multiphoton dissociation spectroscopy. From the IR spectroscopy and from ab initio calculations, they deduced for the $PH{\cdot}W_{n=1-5}$ clusters structures in which the water molecules form H-bonded rings under incorporation of the hydroxyl group of phenol. Leutwyler at al.[145] studied with R2PI the structures, dynamics, and vibrations of cyclic W_3 and its phenyl relative, i.e., $PH{\cdot}W_2$. The results derived gave information on the cluster fluxionality. Gerhards et al.[189] studied $PH{\cdot}W_2$ by ab initio calculations at the HF level and analyzed the intra- and intermolecular vibrations. The OH stretches were in close agreement with the experimental data of Ebata et al.

Further interest in these systems was stimulated by the observation of a proton transfer from the hydroxyl group to proton-accepting solvent subclusters. It occurs with phenol both in the electronically excited (S_1) and in the ionized state. These solvation- and excitation/ionization-dependent acid−base reactions represent under conditions of discrete microsolvation the cluster analogy of condensed-phase acid−base equilibria in solvents of different basicity. Sato and Mikami[167] observed a size-dependent intracluster dissociative proton transfer (dPT) in $PH^+{\cdot}W_n$ similar to that reported first for $TO^+{\cdot}W_n$.[71,179] While dPT from TO^+ to the water subclusters necessitates three water molecules, with PH^+ it sets in with four water molecules. The threshold size was latter confirmed.[75]

The microhydrated phenol was investigated by several groups.[166,228,229] Roth et al.[230] analyzed the system $PH{\cdot}W_n$ in the S_0 state by dispersed fluorescence (n = 3−5) and in the S_1 state by R2PI (n = 5−8, 12), UV/UV spectral hole-burning (n = 2−5), and rotationally resolved LIF (n = 1). For n = 8 they tentatively assigned a particularly stable cubic structure to the water subcluster, which is H-bonded via one of the corner oxygens to the proton-donating phenol. Such an ice-like cubic structure also has been found for W_8[152] and $Bz{\cdot}W_8$. The IR-spectra of the ionized complexes of $PH^+{\cdot}W_n$ (n = 1−4, 7, 8) were determined with R2PI/IR (IR−PARI).[75] For n = 2, a linear structure was deduced. Gerhards et al. did the vibrational analysis of PH·MeOH,[172] and Courty et al.[231] reported results from the ionization, energetics, and geometry of the PH·S complexes (S = H_2O, CH_3-OH, and CH_3OCH_3).

The isomeric clusters of PH·EtOH have been studied by different laser spectroscopic techniques and by ab initio calculations.[104] Three minimum energy structures of anti/gauche OH torsional conformers of the ethanol moiety could be assigned.

The H-bonded cluster of $PH{\cdot}(\text{formic acid})_2$ and $PH{\cdot}(\text{acetic acid})_{n=1-4}$ was studied by Imhof et al.[232,233] with R2PI, IR/R2PI, dispersed fluorescence spectroscopy, and ab initio calculations at the Hartree−Fock level. For n = 2, two isomers could be identified: one with a cyclic structure of the mixed complex and one with an acetic acid dimer attached to phenol.

Some references should be included on the application of IR spectroscopy like ADIR or IR/PIRI to study ions in a specific state. Fujii et al.[121] observed the OH vibrations in cations such as PH^+, p-ethylphenol$^+$,[123] fluorophenol$^+$, methoxyphenol$^+$,[234] and o-cresol$^+$.[235] For the latter three ions the formation of intramolecular H-bonds could be deduced. Gerhards et al.[120] utilized IR/PIRI to study the OH stretches in the two isomers of resorcinol$^+$ (1,3-dihydroxybenzene) and the stretches of the solvent molecules in $PH^+{\cdot}W$[236] and $IN^+{\cdot}W$. In the cluster with indole, these did not couple with the N−H stretch and its overtone.[237]

The singly hydrated noradrenaline analogue 2-amino-1-phenyl-ethanol[105] has been studied in Simons' group with UV−UV hole-burning and IR/R2PI spectroscopy. From the IR spectra, refined experimentally using band contour spectroscopy, and theoretically, using high-level ab initio computation, they got valuable insights into the overall geometry of nonrigid molecular conformers and their hydrated complexes. The results on the monomer, which are probably also relevant for the more complex neurotransmitter, noradrenaline, show that intramolecular H-bonding controls both the conformational structure and the relative conformational abundance. The theoretical study confirms the disruption of the intramolecular H-bond by the first bound water molecule. It also reveals the key role of side-chain flexibility and cooperative effects. The question to which extent a flexible side chain allows the possibility of a π-OH H-bond has also been investigated by the same group.[238] In benzyl alcohol, only a weak π−OH-bond is found. However, a conformer of 2-phenylethanol gains the most energy from the intramolecular H-bond. In 3-phenylpropanol, the constraint implied by the three methylene units allow such a π−OH-bond only under strain in the chain, which reduces the binding energy. Other cluster studied by this group are the 1:1 hydrates of 5-phenyl- and 4-phenylimidazole.[239]

It may be anticipated that in coming years a growing number of chemists, spectroscopists, and theoreticians will analyze several of the classical

photophysical and photochemical processes in structurally well-characterized solvent environments by means of similar spectroscopic methods, as just described.

IV. Summary and Outlook

The main objective of this article was to summarize what is actually known about the structure of microsolvated substituted benzenes and with which methods this information can be extracted. The greatest impact for a structural analysis of aromatic chromophores surrounded by several polar molecules comes certainly from recently developed double-resonance laser spectroscopies, among which the IR/R2PI technique, in particular, provided direct and efficient access to these H-bonded species. Since this method is both structure sensitive by means of the infrared predissociation part and molecule specific and highly sensitive by the R2PI mass spectrometric part, it is very well suited to study molecular clusters.

A more detailed inspection was given to methyl and fluorine substituents for their electron-donating and electron-withdrawing properties, respectively. Thus, the competition between a π−OH H-bond of a solvent subcluster to the aromatic π-system and a σ-type H-bond to its polar binding sites induced by the substituent could be studied as a function of the number of solvent molecules attached. Also, the competition between the solute−solvent and the solvent−solvent interaction was one of the issues. The unique spectroscopic fingerprint of a certain cluster structure is based on IR/R2PI vibrational spectras and on the H-bonding-induced red shifts of the OH and CH vibrations. Also, a novel type of H-bonding was discussed, where the H-bonding induces a blue shift in the stretch frequency of the donating group. However, spectroscopy may only deploy its full potential in combination with the now feasible sophisticated, high-level ab initio methods. The accuracy of the latter may be cross checked by direct comparison of the experimental and calculated vibrational spectra. The advantages and limitations of different approximation methods and of different basis sets may thus be evaluated. From this synergetic interaction of spectroscopy and theory many of the classical concepts of intermolecular interaction may be reexamined. Examples are weak hydrogen bonds of protic donor molecules to the π-electron system of aromatic molecules.

The characterization of a such a microsolvation structure is further stimulated by the solvation-dependent change of chemical reactivity observed for electronically excited or ionized chromophores. Examples are solvation-mediated proton or electron transfer or substitution reactions. The question if the number of molecules or the microsolvation structure is the decisive factor in determining the observed reactivity could not be answered in a general manner. However, in the case of the ion chemistry, the structure of the neutral aggregate proved to be much less relevant than the number of solvent molecules.

While the clusters studied were simple substituted benzenes, the molecular systems that will be studied in the future will certainly be aromatic molecules of biological importance, such as clusters of DNA bases, e.g., base pairs, etc., and of aromatic amino acids, etc. Thus, many of the concepts and methods developed during the last few years of intense work on relatively simple cluster systems in the gas phase may allow a shift of the frontiers to more complicated molecular systems. The progress in this direction is intimately connected with further advances in theoretical methods and a reliable knowledge as to their accuracy and range. Hence, verification of theoretical methods by the interpretation or even prediction of spectroscopic results will be one of few ways to progress further into both the complicated and simple world of intermolecular interactions.

V. Acknowledgments

This work was supported by the DFG Forschungsschwerpunkt “Molekulare Cluster” and by the J. W. Goethe-Universität Frankfurt. I thank Professor K. S. Kim, Dr. Tarakeshwar, Professor P. Hobza, Dr. Z. Havlas, and V. Spirko for their excellent theoretical support of our experimental work and for a stimulating collaboration. I am also very indebted to many people from my group for doing the experiments and their help in preparing this article: Drs. H.-D. Barth, K. Buchhold, S. Djafari, G. Lembach, U. Lommatzsch, Ch. Riehn, and A. Steiger and Dipl. Chem. B. Reimann and S. Vaupel. Financial support by the “Fonds der chemischen Industrie” is also acknowledged.

VI. References

(1) Levy, D. H. *Adv. Chem. Phys.* **1981**, *47*, 323.
(2) Jortner, J. *Large and Finite Systems*; Reidel: Dortrecht, 1987.
(3) Jortner, J.; Even, U.; Goldberg, A.; Schek, I.; Raz, T.; Levine, R. D. *Surf. Rev. Lett.* **1996**, *3*, 263−280.
(4) Castleman, A. W., Jr.; Wei, S. *Annu. Rev. Phys. Chem.* **1994**, *45*, 685−719.
(5) Castleman, A. W., Jr.; Bowen, K. H. *J. Phys. Chem.* **1996**, *100*, 12911−12944.
(6) *Chemical reactions in clusters*; Bernstein, E. R., Ed.; Oxford University Press: New York, Oxford, 1996.
(7) Brutschy, B. *J. Phys. Chem.* **1990**, *94*, 8637.
(8) Brutschy, B. *Chem. Rev.* **1992**, *92*, 1567.
(9) Maeyama, T.; Mikami, M. *J. Am. Chem. Soc.* **1988**, *110*, 7238.
(10) Martrenchard-Barra, S.; Dedonder-Lardeux, C.; Jouvet, C.; Rockland, U. *J. Phys. Chem.* **1995**, *99*, 13716−13730.
(11) Dedonder-Lardeux, C.; Jouvet, C.; Martrenchard, S.; Solgadi, D.; McCombie, J.; Howells, B. D.; Palmer, T. F.; Subaricleitis, A.; Monte, C.; Rettig, W.; Zimmermann, P. *Chem. Phys.* **1995**, *191*, 271−287.
(12) Cheshnovsky, O.; Leutwyler, S. *Chem. Phys. Lett.* **1985**, *121*, 1.
(13) Jortner, J. *J. Chim. Phys. Phys.-Chim. Biol.* **1995**, *92*, 205−225.
(14) Schmidt, M.; Kusche, R.; von Issendorff, B.; Haberland, H. *Nature* **1998**, *393*, 238−240.
(15) Dimopoulou-Rademann, O.; Rademann, K.; Bisling, P.; B., B.; Baumgärtel, H. *Ber. Bunsen-Ges. Phys. Chem.* **1984**, *88*, 215.
(16) Cheshnovsky, O.; Leutwyler, S. *J. Chem. Phys.* **1988**, *88*.
(17) Papanikolas, J. M.; Vorsa, V.; Nadal, M. E.; Campagnola, P. J.; Buchenau, H. K.; Lineberger, W. C. *J. Chem. Phys.* **1993**, *99*, 8733−8750.
(18) Nadal, M. E.; Kleiber, P. D.; Lineberger, W. C. *J. Chem. Phys.* **1996**, *105*, 504−514.
(19) Greenblatt, B. J.; Zanni, M. T.; Neumark, D. M. *J. Chem. Phys.* **1999**, *111*, 10566−10577.
(20) Seinfeld, J. H. *Science* **1991**, *243*, 745.
(21) Dougherty, J. C. *Chem. Rev.* **1997**, *97*, 1303−1324.
(22) Burley, S. K.; Petesko, G. A. *FEBS Lett.* **1986**, *203*, 139−143.
(23) Felker, P. M.; Maxton, P. M.; Schaeffer, M. W. *Chem. Rev.* **1994**, *94*, 1787−1805.
(24) Neusser, H. J.; Krause, H. *Chem. Rev.* **1994**, *94*, 1829−1843.
(25) Zwier, T. S. *Annu. Rev. Phys. Chem.* **1996**, *47*, 205−241.
(26) Millie, P.; Brenner, V. *J. Chim. Phys. Phys.-Chim. Biol.* **1995**, *92*, 428−444.

(27) Hobza, P.; Zahradnik, R. *Collect. Czech. Chem. Commun.* **1993**, *58*, 1465−1475.
(28) Pratt, D. W. *Annu. Rev. Phys. Chem.* **1998**, *49*, 481−530.
(29) Bernstein, E. R. *Annu. Rev. Phys. Chem.* **1995**, *46*, 197−222.
(30) Castleman, A. W., Jr.; Hobza, P. *Chem. Rev.* **1994**, *94*, 1721−1722.
(31) Märk, T. D.; Castleman, A. W., Jr. *Adv. At. Mol. Phys.* **1985**, *20*.
(32) Buck, U. *Clusters of Atoms and Molecules*; Springer-Verlag: Heidelberg, 1992.
(33) *Chem. Rev.* **1986**, *86*, 491−657.
(34) *Chem. Rev.* **1988**, *88*, 813−988.
(35) *Chem. Rev.* **1994**, *94*, 1721−2160.
(36) Ebata, T.; Fujii, A.; Mikami, N. *Int. Rev. Phys. Chem.* **1998**, *17*, 331−361.
(37) March, J. *Advanced Organic Chemistry*, 4th ed.; J. Wiley & Sons: New York, 1992.
(38) Tarakeshwar, P.; Kim, K. S.; Brutschy, B. *J. Chem. Phys.* **1999**, *110*, 8501−8512.
(39) Tarakeshwar, P.; Kim, K. S.; Brutschy, B. *J. Chem. Phys.* **2000**, *112*, 1769.
(40) Hobza, P.; Spirko, V.; Selzle, H. L.; Schlag, E. W. *J. Phys. Chem.* **1998**, *102*, 2501−2504.
(41) *Atomic and Molecular Beam Methods*; Scoles, G., Ed.; Oxford University Press: New York, Oxford, 1988.
(42) Buchhold, K.; Reimann, B.; Djafari, S.; Barth, H.-D.; Brutschy, B.; Tarakeswar, P.; Kim, K. S. *J. Chem. Phys.* **2000**, *112*, 1844−1858.
(43) Djafari, S.; Lembach, G.; Barth, H. D.; Brutschy, B. *J. Chem. Phys.* **1997**, *107*, 10573−10581.
(44) Lommatzsch, U.; Gerlach, A.; Lahmann, C.; Brutschy, B. *J. Phys. Chem.* **1998**, *102*, 6421−6435.
(45) Buck, U.; Meyer, H. *Phys. Rev. Lett.* **1984**, *52*, 109.
(46) Gutowsky, H. S.; Keen, J. D.; Germann, T. C.; Emilsson, T.; Augspurger, J. D.; Dykstra, C. E. *J. Chem. Phys.* **1993**, *98*, 6801−6809.
(47) Jackel, J. G.; Schmid, R.; Jones, H.; Nakanaga, T.; Takeo, H. *Chem. Phys.* **1997**, *215*, 291−298.
(48) Rodham, D. A.; Suzuki, S.; Suenram, R. D.; Lovas, F. J.; Dasgupta, S.; Goddard, W. A.; Blake, G. A. *Nature* **1993**, *362*, 735−737.
(49) Dahmen, U.; Stahl, W.; Dreizler, H. *Ber. Bunsen-Ges. Phys. Chem.* **1994**, *98*, 970−974.
(50) Yang, X.; Kerstel, E. R. T.; Scoles, G.; Bemish, R. J.; Miller, R. E. *J. Chem. Phys.* **1995**, *103*, 8828−8839.
(51) Caminati, W.; di Bernardo, S. *J. Mol. Struct.* **1990**, *240*, 253.
(52) Spoerel, U.; Stahl, W.; Caminati, W.; Favero, P. G. *Chem.-A Eur. J.* **1998**, *4*, 1974−1981.
(53) Felker, P. M.; Zewail, A. H. *Femtochemistry*; VCH: Weinheim, 1995.
(54) Riehn, C.; Weichert, A.; Lommatzsch, U.; Zimmermann, M.; Brutschy, B. *J. Chem. Phys.* **2000**, *112*, 3650.
(55) Ohline, S. M.; Romascan, J.; Felker, P. M. *Chem. Phys. Lett.* **1993**, *207*, 563−568.
(56) Benharash, P.; Gleason, M. J.; Felker, P. M. *J. Phys. Chem.* **1999**, *103*, 1442−1446.
(57) Riehn, C.; Weichert, A.; Brutschy, B. *P. C. C. P.* **2000**, *2*, 1873−1875.
(58) Felker, P. M. *J. Phys. Chem.* **1992**, *96*, 7844.
(59) Topp, M. R. *Int. Rev. Phys. Chem.* **1993**, *12*.
(60) Connell, L. L.; Ohline, S. M.; Joireman, P. W.; Corcoran, T. C.; Felker, P. M. *J. Chem. Phys.* **1992**, *96*, 2585.
(61) Joireman, P. W.; Connell, L. L.; Ohline, S. M.; Felker, P. M. *J. Phys. Chem.* **1991**, *95*, 4935.
(62) Magnera, T. F.; Sammond, D. M.; Michl, J. *Chem. Phys. Lett.* **1993**, *211*, 378−380.
(63) Andrews, P. M.; Pryor, B. A.; Berger, M. B.; Palmer, P. M.; Topp, M. R. *J. Phys. Chem.* **1997**, *101*, 6222−6232.
(64) Fujiwara, T.; Fujimura, Y.; Kajimoto, O. *Chem. Phys. Lett.* **1996**, *261*, 201−207.
(65) Riehn, C.; Weichert, A.; Zimmermann, M.; Brutschy, B. *Chem. Phys. Lett.* **1999**, *299*, 103−109.
(66) Boesl, U.; Neusser, H. J.; Schlag, E. W. *Z. Naturforsch.* **1978**, *33a*, 1546.
(67) Letokhov, V. S. *Laser Photoionization Spectroscopy*; Academic Press: New York, 1987.
(68) Fung, K. H.; Selzle, H. L.; Schlag, E. W. *Z. Naturforsch.* **1981**, *36a*, 1338.
(69) Hopkins, J. B.; Powers, D. E.; Smalley, R. E. *J. Phys. Chem.* **1981**, *85*, 3739.
(70) Rademann, K.; Brutschy, B.; Baumgärtel, H. *Chem. Phys.* **1983**, *80*, 129.
(71) Brutschy, B.; Janes, C.; Eggert, J. *Ber. Bunsen-Ges. Phys. Chemie* **1988**, *92*, 74.
(72) Brutschy, B.; C., J.; Eggert, J. *Ber. Bunsen-Ges. Phys. Chemie* **1988**, *92*, 435.
(73) Abrahamson, E.; Field, R. W.; Imre, D.; Innes, K. K.; Kinsey, J. L. *J. Chem. Phys.* **1985**, *83*, 453.
(74) Lipert, R. J.; Colson, S. D. *Chem. Phys. Lett.* **1989**, *161*, 303.
(75) Kleinermanns, K.; Janzen, C.; Spangenberg, D.; Gerhards, M. *J. Phys. Chem.* **1999**, *103*, 5232−5239.
(76) Demtröder, W. *Laserspektroskopie*; Springer-Verlag: Berlin, Heidelberg, 1991.
(77) Huisken, F.; Kulcke, A.; Voelkel, D.; Laush, C.; Lisy, J. M. *Appl. Phys. Lett.* **1993**, *62*, 805−807.
(78) Page, R. H.; Frey, S. G.; Shen, Y. R.; Lee, Y. T. *Chem. Phys. Lett.* **1984**, *106*, 373.
(79) Huisken, F.; Kaloudis, M.; Kulcke, A. *J. Chem. Phys.* **1996**, *104*, 17−25.
(80) Okumura, M.; Yeh, L. I.; Myers, J. D.; Lee, Y. T. *J. Phys. Chem.* **1990**, *94*, 3416.
(81) Selegue, T. J.; Cabarcos, O. M.; Lisy, J. M. *J. Chem. Phys.* **1994**, *100*, 4790−4796.
(82) Weinheimer, C. J.; Lisy, J. M. *J. Chem. Phys.* **1996**, *105*, 2938−2941.
(83) Ayotte, P.; Bailey, C. G.; Kim, J.; Johnson, M. A. *J. Chem. Phys.* **1998**, *108*, 444−449.
(84) Ayotte, P.; Weddle, G. H.; Kim, J.; Johnson, M. A. *Chem. Phys.* **1998**, *239*, 485−491.
(85) Page, R. H.; Shen, Y. R.; Lee, Y. T. *J. Chem. Phys.* **1989**, *88*, 4621.
(86) Riehn, C.; Lahmann, C.; Wassermann, B.; Brutschy, B. *Ber. Bunsen-Ges. Phys. Chem.* **1992**, *96*, 1161.
(87) Riehn, C.; Lahmann, C.; Wassermann, B.; Brutschy, B. *Chem. Phys. Lett.* **1992**, *197*, 443.
(88) Brutschy, B.; Eggert, J.; Janes, C.; Baumgärtel, H. *J. Phys. Chem.* **1990**, *95*, 5041.
(89) Maeyama, T.; Mikami, N. *J. Phys. Chem.* **1991**, *95*, 7197.
(90) Huisken, F.; Stemmler, M. *Chem. Phys. Lett.* **1988**, *144*, 391.
(91) Huisken, F.; Kulcke, A.; Laush, C.; Lisy, J. M. *J. Chem. Phys.* **1991**, *95*, 3924.
(92) Fujii, A.; Okuyama, S.; Iwasaki, A.; Maeyama, T.; Ebata, T.; Mikami, N. *Chem. Phys. Lett.* **1996**, *256*, 1−7.
(93) Pimentel, G. C.; McClellan, A. L. *The Hydrogen Bond*; Freeman: San Francisco, 1960.
(94) Engdahl, A.; Nelander, B.; Astrand, P. O. *J. Chem. Phys.* **1993**, *99*, 4894−4907.
(95) Bellamy, L. J. *Advances in Infrared Group Frequencies*; Methuen: London, 1968.
(96) Kleeberg, H.; Eiseberg, C.; Zinn, T. *J. Mol. Struct.* **1990**, *240*, 175.
(97) Scherer, J. J.; Paul, J. B.; Okeefe, A.; Saykally, R. J. *Chem. Rev.* **1997**, *97*, 25−51.
(98) Pimentel, G. C.; McClellan, A. L. *Annu. Rev. Phys. Chem.* **1971**, *22*, 347.
(99) Jeffrey, G. A. *An Introduction to Hydrogen Bonding*; Oxford University Press: New York, Oxford, 1997.
(100) *Molecular interactions: From van der Waals to strongly bound complexes*; Scheiner, S., Ed.; John Wiley & Sons: Chichester, New York, Weinheim, 1997.
(101) Vanderheyden, L.; Vandenbrande, R.; Zeegers-Huyskens, T. *Spectrosc. Lett.* **1989**, *72*, 686.
(102) Tanabe, S.; Ebata, T.; Fujii, M.; Mikami, N. *Chem. Phys. Lett.* **1993**, *215*, 347−352.
(103) Pribble, R. N.; Zwier, T. S. *Science* **1994**, *265*, 75−79.
(104) Spangenberg, D.; Imhof, P.; Roth, W.; Janzen, C.; Kleinermanns, K. *J. Phys. Chem.* **1999**, *103*, 5918−5924.
(105) Graham, R. J.; Kroemer, R. T.; Mons, M.; Robertson, E. G.; Snoek, L. C.; Simons, J. P. *J. Phys. Chem.* **1999**, *103*, 9706−9711.
(106) Ebata, T.; Mizuochi, N.; Watanabe, T.; Mikami, N. *J. Phys. Chem.* **1996**, *100*, 546−550.
(107) Hartland, G. V.; Henson, B. F.; Venturo, V. A.; Felker, P. M. *J. Phys. Chem.* **1992**, *96*, 1164.
(108) Ishikawa, S.; Ebata, T.; Mikami, N. *J. Chem. Phys.* **1999**, *110*, 9504−9515.
(109) Nakanaga, T.; Ito, F.; Miyawaki, J.; Sugawara, K.; Takeo, H. *Chem. Phys. Lett.* **1996**, *261*, 414−420.
(110) Schmid, R. P.; Chowdhury, P. K.; Miyawaki, J.; Ito, F.; Sugawara, K.; Nakanaga, T.; Takeo, H.; Jones, H. *Chem. Phys.* **1997**, *218*, 291−300.
(111) Nakanaga, T.; Sugawara, K.; Kawamata, K.; Ito, F. *Chem. Phys. Lett.* **1997**, *267*, 491−495.
(112) Sasaki, T.; Mikami, N. *Chem. Phys. Lett.* **1993**, *209*, 379−382.
(113) Mikami, N.; Sato, S.; Ishigaki, M. *Chem. Phys. Lett.* **1993**, *202*, 431−436.
(114) Johnson, P. M.; Zhu, L. C. *Int. J. Mass Spectrosc. Ion Processes* **1994**, *131*, 193−209.
(115) Goode, J. G.; Leclaire, J. E.; Johnson, P. M. *Int. J. Mass Spectrosc. Ion Processes* **1996**, *159*, 49−64.
(116) Schlag, E. W.; Peatman, W. B.; Müller-Dethlefs, K. *J. Electron Spectrosc. Relat. Phenom.* **1993**, *66*, 139−149.
(117) Krause, H.; Neusser, H. J. *J. Photochem. Photobiol., A-Chem.* **1994**, *80*, 73−83.
(118) Lembach, G.; Brutschy, B. *Chem. Phys. Lett.* **1997**, *273*, 421−428.
(119) Goode, J. G.; Hofstein, J. D.; Johnson, P. M. *J. Chem. Phys.* **1997**, *107*, 1703−1716.

(120) Gerhards, M.; Schiwek, M.; Unterberg, C.; Kleinermanns, K. *Chem. Phys. Lett.* **1998**, *297*, 515−522.
(121) Fujii, A.; Iwasaki, A.; Ebata, T.; Mikami, N. *J. Phys. Chem.* **1997**, *101*, 5963−5965.
(122) Fujii, A.; Iwasaki, A.; Mikami, N. *Chem. Lett.* **1997**, 1099−1100.
(123) Fujii, A.; Fujimaki, E.; Ebata, T.; Mikami, N. *Chem. Phys. Lett.* **1999**, *303*, 289−294.
(124) Lembach, G. Dissertation, Frankfurt/Main, 1998.
(125) Dopfer, O.; Reiser, G.; Müller-Dethlefs, K.; Schlag, E. W.; Colson, S. D. *J. Chem. Phys.* **1994**, *101*, 974−989.
(126) Müller-Dethlefs, K.; Schlag, E. W. *Angew. Chem., Int. Ed. Engl.* **1998**, *37*, 1346−1374.
(127) Helm, R. M.; Clara, M.; Grebner, T. L.; Neusser, H. J. *J. Phys. Chem.* **1998**, *102*, 3268−3272.
(128) Braun, J. E.; Grebner, T. L.; Neusser, H. J. *J. Phys. Chem.* **1998**, *102*, 3273−3278.
(129) Schutz, M.; Burgi, T.; Leutwyler, S.; Fischer, T. *J. Chem. Phys.* **1993**, *98*, 3763−3776.
(130) Helm, R. M.; Vogel, H. P.; Neusser, H. J. *J. Chem. Phys.* **1998**, *108*, 4496−4504.
(131) Gerhards, M.; Schmitt, M.; Kleinermanns, K.; Stahl, W. *J. Chem. Phys.* **1996**, *104*, 967−971.
(132) Levitt, M.; Perutz, M. F. *J. Mol. Biol.* **1988**, *201*, 751.
(133) Perutz, M. *The Chemical Bond*; Academic Press: New York, 1992.
(134) Engdahl, A.; Nelander, B. *J. Phys. Chem.* **1985**, *89*, 2860.
(135) Klemperer, W. *Nature* **1993**, *362*, 698.
(136) Gotch, A. J.; Garrett, A. W.; Severance, D. L.; Zwier, T. S. *Chem. Phys. Lett.* **1991**, *178*, 121−129.
(137) Suzuki, S.; Green, P. G.; Bumgarner, R. E.; Dasgupta, S.; Goddard, W. A. I.; Blake, G. A. *Science* **1992**, *257*, 942.
(138) Gutowsky, H. S.; Emilsson, T.; Arunan, E. *J. Chem. Phys.* **1993**, *99*, 4883−4893.
(139) Pribble, R. N.; Hagemeister, F. C.; Zwier, T. S. *J. Chem. Phys.* **1997**, *106*, 2145−2157.
(140) Xantheas, S. S.; Dunning, T. H. *J. Chem. Phys.* **1993**, *99*, 8774−8792.
(141) Xantheas, S. S. *Philos. Mag. B−Phys. Condens. Matter Struct. Electron. Opt. Magn. Prop.* **1996**, *73*, 107−115.
(142) Xantheas, S. S.; Dunning, T. H. *J. Chem. Phys.* **1993**, *98*, 8037−8040.
(143) Xantheas, S. S. *J. Chem. Phys.* **1994**, *100*, 7523−7534.
(144) Schutz, M.; Burgi, T.; Leutwyler, S.; Burgi, H. B. *J. Chem. Phys.* **1994**, *100*, 1780.
(145) Leutwyler, S.; Burgi, T.; Schutz, M.; Taylor, A. *Faraday Discuss.* **1994**, 285−297.
(146) Graf, S.; Leutwyler, S. *J. Chem. Phys.* **1998**, *109*, 5393−5403.
(147) Graf, S.; Mohr, W.; Leutwyler, S. *J. Chem. Phys.* **1999**, *110*, 7893−7908.
(148) Huisken, F.; Kaloudis, M.; Kulcke, A.; Voelkel, D. *Infrared Phys. Technol.* **1995**, *36*, 171−178.
(149) Augspurger, J. D.; Dykstra, C. E.; Zwier, T. S. *J. Phys. Chem.* **1993**, *97*, 980−984.
(150) Kim, J.; Kim, K. S. *J. Chem. Phys.* **1998**, *109*, 5886−5895.
(151) Gruenloh, C. J.; Carney, J. R.; Arrington, C. A.; Zwier, T. S.; Fredericks, S. Y.; Jordan, K. D. *Science* **1997**, *276*, 1678−1681.
(152) Buck, U.; Ettischer, I.; Melzer, M.; Buch, V.; Sadlej, J. *Phys. Rev. Lett.* **1998**, *80*, 2578−2581.
(153) Gruenloh, C. J.; Carney, J. R.; Hagemeister, F. C.; Zwier, T. S.; Wood, J. T. I.; Jordan, K. D. Submitted to *J. Chem. Phys.*
(154) Huisken, F.; Kaloudis, M.; Koch, M.; Werhahn, O. *J. Chem. Phys.* **1996**, *105*, 8965−8968.
(155) Tschumper, G. S.; Gonzales, J. M.; Schaefer, H. F., III. *J. Chem. Phys.* **1999**, *111*, 3027−3034.
(156) Gruenloh, C. J.; Florio, G. M.; Carney, J. R.; Hagemeister, F. C.; Zwier, T. S. *J. Phys. Chem.* **1999**, *103*, 496−502.
(157) Hagemeister, F. C.; Gruenloh, C. J.; Zwier, T. S. *Chem. Phys.* **1998**, *239*, 83−96.
(158) Kim, K.; Jordan, K. D.; Zwier, T. S. *J. Am. Chem. Soc.* **1994**, *116*, 11568−11569.
(159) Fredericks, S. Y.; Jordan, K. D.; Zwier, T. S. *J. Phys. Chem.* **1996**, *100*, 7810−7821.
(160) Fredericks, S. Y.; Pedulla, J. M.; Jordan, K. D.; Zwier, T. S. *Theor. Chem. Acc.* **1997**, *96*, 51−55.
(161) Maes, G.; Smets, J.; Adamowicz, L.; McCarthy, W.; Van Bael, M. K.; Houben, L.; Schoone, K. *J. Mol. Struct.* **1997**, *410−411*, 315−322.
(162) Smets, J.; McCarthy, W.; Maes, G.; Adamowicz, L. *J. Mol. Struct.* **1999**, *476*, 27−43.
(163) Hobza, P. Private communication.
(164) Riehn, C.; Lahmann, C.; Brutschy, B.; Baumgärtel, H. *Ber. Bunsen-Ges. Phys. Chem.* **1992**, *96*, 1164.
(165) Li, S.; Bernstein, E. R. *J. Chem. Phys.* **1992**, *97*, 792.
(166) Hineman, M. F.; Kelley, D. F.; Bernstein, E. R. *J. Chem. Phys.* **1993**, *99*, 4533−4538.
(167) Sato, S.; Mikami, N. *J. Phys. Chem.* **1996**, *100*, 4765−4769.
(168) Ebata, T.; Fujii, A.; Mikami, N. *Int. J. Mass Spectrosc. Ion Processes* **1996**, *159*, 111−124.
(169) Iwasaki, A.; Fujii, A.; Watanabe, T.; Ebata, T.; Mikami, N. *J. Phys. Chem.* **1996**, *100*, 16053−16057.
(170) Fujii, A.; Iwasaki, A.; Yoshida, K.; Ebata, T.; Mikami, N. *J. Phys. Chem.* **1997**, *101*, 1798−1803.
(171) Guchhait, N.; Ebata, T.; Mikami, N. *J. Chem. Phys.* **1999**, *111*, 8438−8447.
(172) Gerhards, M.; Beckmann, K.; Kleinermanns, K. *Z. Phys. D* **1994**, *29*, 223−229.
(173) Schmitt, M.; Muller, H.; Kleinermanns, K. *Chem. Phys. Lett.* **1994**, *218*, 246−248.
(174) Schiefke, A.; Deusen, C.; Jacoby, C.; Gerhards, M.; Schmitt, M.; Kleinermanns, K.; Hering, P. *J. Chem. Phys.* **1995**, *102*, 9197−9204.
(175) Jacoby, C.; Roth, W.; Schmitt, M.; Janzen, C.; Spangenberg, D.; Kleinermanns, K. *J. Phys. Chem.* **1998**, *102*, 4471−4480.
(176) Janzen, C.; Spangenberg, D.; Roth, W.; Kleinermanns, K. *J. Chem. Phys.* **1999**, *110*, 9898−9907.
(177) Gerhards, M.; Perl, W.; Kleinermanns, K. *Chem. Phys. Lett.* **1995**, *240*, 506−512.
(178) Barth, H. D.; Buchhold, K.; Djafari, S.; Reimann, B.; Lommatzsch, U.; Brutschy, B. *Chem. Phys.* **1998**, *239*, 49−64.
(179) Foltin, M.; Stueber, G. J.; Bernstein, E. R. *J. Chem. Phys.* **1998**, *109*, 4342−4360.
(180) Pribble, R. N.; Zwier, T. S. *Faraday Discuss.* **1994**, 229−241.
(181) Gregory, J. K.; Clary, D. C. *Mol. Phys.* **1996**, *88*, 33−52.
(182) Kim, K. S.; Lee, J. Y.; Choi, H. S.; Kim, J. S.; Jang, J. H. *Chem. Phys. Lett.* **1997**, *265*, 497−502.
(183) Sorenson, J. M.; Gregory, J. K.; Clary, D. C. *J. Chem. Phys.* **1997**, *106*, 849−863.
(184) Tarakeshwar, P.; Choi, H. S.; Lee, S. J.; Lee, J. Y.; Kim, K. S.; Ha, T. K.; Jang, J. H.; Lee, J. G.; Lee, H. *J. Chem. Phys.* **1999**, *111*, 5838−5850.
(185) Courty, A.; Mons, M.; Dimicoli, I.; Gaigeot, M.; Brenner, V.; de Pujo, P.; Millie, P. *J. Phys. Chem. A* **1998**, *102*, 6590.
(186) Reimann, B.; Vaupel, S.; Riehn, C.; Brutschy, B. Unpublished data.
(187) Hagemeister, F. C.; Gruenloh, C. J.; Zwier, T. S. *J. Phys. Chem.* **1998**, *102*, 82−94.
(188) Ebata, T.; Watanabe, T.; Mikami, N. *J. Phys. Chem.* **1995**, *99*, 5761−5764.
(189) Gerhards, M.; Kleinermanns, K. *J. Chem. Phys.* **1995**, *103*, 7392−7400.
(190) Paul, J. B.; Provencal, R. A.; Chapo, C.; Roth, K.; Casaes, R.; Saykally, R. J. *J. Phys. Chem.* **1999**, *103*, 2972−2974.
(191) Dunitz, J. D.; Taylor, R. *Chem. Eur. J.* **1997**, *3*, 89.
(192) Vishnumurthy, K.; Row, T. N. G.; Venkatesan, K. *J. Chem. Soc., Perkin Trans.* **1996**, *2*, 1475.
(193) Hayashi, N.; Mori, T.; Matsumoto, K. *J. Chem. Soc., Chem. Commun.* **1998**, 1905.
(194) Caminati, W.; Melandri, S.; Rossi, I.; Favero, P. G. *J. Am. Chem. Soc.* **1999**, *121*, 10098−10101.
(195) Danten, Y.; Tassaing, T.; Besnard, M. *J. Phys. Chem.* **1999**, *103*, 3530−3534.
(196) Lee, J. Y.; Hahn, O.; Lee, S. J.; Choi, H. S.; Shim, H. S.; Mhin, B. J.; Kim, K. S. *J. Phys. Chem.* **1995**, *99*, 1913−1918.
(197) Lee, J. Y.; Hahn, O.; Lee, S. J.; Mhin, B. J.; Lee, M. S.; Kim, K. S. *J. Phys. Chem.* **1995**, *99*, 2262−2266.
(198) Djafari, S.; Lembach, G.; Barth, H. D.; Brutschy, B. *Z. Phys. Chem.* **1996**, *195*, 253−272.
(199) Buchhold, K. Dissertation, Frankfurt/Main, 2000.
(200) Martrenchard, S.; Jouvet, C.; Lardeux-Dedonder, C.; Solgadi, D. *J. Chem. Phys.* **1991**, *95*, 9186−9191.
(201) Buchhold, K.; Reimann, B.; Djafari, S.; Barth, H. D.; Brutschy, B.; Tarakeshwar, P.; Kim, K. *J. Chem. Phys.* **2000**, *112*, 1844.
(202) Tarakeshwar, P.; Kim, K. S. Unpublished data, 2000.
(203) Riehn, C.; Buchhold, K.; Reimann, B.; Djafari, S.; Barth, H.-D.; Brutschy, B.; Tarakeshwar, P.; Kim, K. S. *J. Chem. Phys.* **2000**, *112*, 1170−1177.
(204) Silvi, B.; Wiecorek, R.; Latajka, Z.; Alikhani, M. E.; Dkhissi, A.; Bouteiller, Y. *J. Chem. Phys.* **199**, *111*, 6671.
(205) Brenner, V.; Martrenchard-Barra, S.; Millie, P.; Dedonder-Lardeux, C.; Jouvet, C.; Sogadi, D. *J. Phys. Chem.* **1995**, *99*, 5848−5860.
(206) Tsymbal, I. F.; Ryltsev, E. V.; Bodeskul, I. E.; Lysak, B. G. *Khim. Fiz.* **1993**, *12*, 988.
(207) Boldeskul, I. E.; Tsymbal, I. F.; Ryltsev, E. V.; Latajka, Z.; Barnes, A. J. *J. Mol. Struct.* **1997**, *436*, 167.
(208) Nishio, M.; Hirota, M.; Umezawa, Y. *The CH/pi Interaction*; Wiley: Chichester, 1998.
(209) Umezawa, Y.; Tsuboyama, S.; Takahashi, H.; Uzawa, J.; Nishio, M. *Tetrahedron* **1999**, *55*, 10047−10056.
(210) Reeves, L. W.; Schneider, W. G. *Can. J. Chem.* **1957**, *35*, 251.
(211) Hobza, P.; Spirko, V.; Havlas, Z.; Buchhold, K.; Reimann, B.; Barth, H. D.; Brutschy, B. *Chem. Phys. Lett.* **1999**, *299*, 180−186.
(212) Cubero, E.; Orozco, M.; Hobza, P.; Luque, F. J. *J. Phys. Chem.* **1999**, *103*, 6394−6401.
(213) Reimann, B.; Vaupel, S.; Buchhold, K.; Riehn, C.; Brutschy, B. Unpublished data.

(214) Reimann, B.; Vaupel, S.; Brutschy, B.; Havlas, Z.; Spirko, V.; Hobza, P. Submitted *J. Am. Chem. Soc.*
(215) Sugawara, K.; Miyawaki, J.; Nakanaga, T.; Takeo, H.; Lembach, G.; Djafari, S.; Barth, H. D.; Brutschy, B. *J. Phys. Chem.* **1996**, *100*, 17145−17147.
(216) Nakanaga, T.; Chowdhury, P. K.; Ito, F.; Sugawara, K.; Takeo, H. *J. Mol. Struct.* **1997**, *413*, 205−209.
(217) Kawamata, K.; Chowdhury, P. K.; Ito, F.; Sugawara, K.; Nakanaga, T. *J. Phys. Chem.* **1998**, *102*, 4788−4793.
(218) Nakanaga, T.; Ito, F. *J. Phys. Chem.* **1999**, *103*, 5440−5445.
(219) Nakanaga, T.; Kawamata, K.; Ito, F. *Chem. Phys. Lett.* **1997**, *279*, 309−314.
(220) Carney, J. R.; Hagemeister, F. C.; Zwier, T. S. *J. Chem. Phys.* **1998**, *108*, 3379−3382.
(221) Kortner, T. M.; Pratt, D. W.; Küppers, J. *J. Phys. Chem.* **1998**, *102*, 2A, 7211.
(222) Carney, J. R.; Zwier, T. S. *J. Phys. Chem. A*, in print 1999.
(223) Mordzinski, A.; Sobolewski, A. L.; Levy, D. H. *J. Phys. Chem.* **1997**, *101*, 8221−8226.
(224) Kobayashi, T.; Kajimoto, O. *Res. Chem. Interm.* **1998**, *24*, 785−802.
(225) Helm, R. M.; Vogel, H. P.; Neusser, H. J.; Storm, V.; Consalvo, D.; Dreizler, H. *Z. Naturforsch.* **1997**, *52*, 655−664.
(226) Zwier, T. S. *Adv. Molec. Vibr. Collision Dynam.* **1998**, *3*, 249−280.
(227) Watanabe, T.; Ebata, T.; Tanabe, S.; Mikami, N. *J. Chem. Phys.* **1996**, *105*, 408−419.
(228) Kleinermanns, K.; Gerhards, M.; Schmitt, M. *Ber. Bunsen-Ges. Phys. Chem.* **1997**, *101*, 1785−1798.
(229) Martrenchard-Barra, S.; Dedonder-Lardeux, C.; Jouvet, C.; Solgadi, D.; Vervloet, M.; Gregoire, G.; Dimicoli, I. *Chem. Phys. Lett.* **1999**, *310*, 173−179.
(230) Roth, W.; Schmitt, M.; Jacoby, C.; Spangenberg, D.; Janzen, C.; Kleinermanns, K. *Chem. Phys.* **1998**, *239*, 1−9.
(231) Courty, A.; Mons, M.; Dimicoli, I.; Piuzzi, F.; Brenner, V.; Millie, P. *J. Phys. Chem.* **1998**, *102*, 4890−4898.
(232) Imhof, P.; Roth, W.; Janzen, C.; Spangenberg, D.; Kleinermanns, K. *Chem. Phys.* **1999**, *242*, 141−151.
(233) Imhof, P.; Roth, W.; Janzen, C.; Spangenberg, D.; Kleinermanns, K. *Chem. Phys.* **1999**, *242*, 153−159.
(234) Fujimaki, E.; Fujii, A.; Ebata, T.; Mikami, N. *J. Chem. Phys.* **1999**, *110*, 4238−4247.
(235) Fujii, A.; Fujimaki, E.; Ebata, T.; Mikami, N. *J. Am. Chem. Soc.* **1998**, *120*, 13256−13257.
(236) Unterberg, C.; Jansen, A.; Gerhards, M. Submitted to *Chem. Phys. Lett.*
(237) Gerhards, M.; Unterberg, C.; Jansen, A.; Kleinermanns, K. Submitted to *Chem. Phys. Lett.*
(238) Mons, M.; Robertson, E. G.; Simons, J. P. *J. Phys. Chem.* **2000**, *104*, 1430−1437.
(239) Hockridge, M. R.; Roberson, E. G.; Simons, J. P. *Chem. Phys. Lett.* **1999**, *302*, 538−548.
(240) Pribble, R. N.; Garrett, A. W.; Haber, K.; Zwier, T. S. *J. Chem. Phys.* **1995**, *103*, 531−544.
(241) Tarakeshwar, P.; Kim, K. S.; Brutschy, B. Unpublished data.
(242) Herzberg, G. *Molecular Spectra and Molecular Structure*; van Nostrand Reinhold: New York, 1945.
(243) Shimanouchi, T. *Tables of Molecular Vibrational Frequencies*; USGPO: Washington, DC, 1972.
(244) Coussan, S.; Bakkas, N.; Loutellier, A.; Perchard, J. P.; Racine, S. *Chem. Phys. Lett.* **1994**, *217*, 123.
(245) Xu, L.; Want, X.; al., e. *J. Mol. Spectrosc.* **1997**, *186*, 158.
(246) Dübal, H. R.; Quack, M. *Chem. Phys. Lett* **1981**, *81*, 439.
(247) Tarakeshwar, P.; Kim, K. S.; Brutschy, B. *J. Chem. Phys.* submitted.

CR990055N